

Supporting Information for:

Stapled beta-hairpins featuring 4-mercaptoproline

Jennifer R. Pace, Bryan J. Lampkin, Charles Abakah, Adam Moyer, Jiayuan Miao, Kirsten Deprey, Robert A. Cerulli, Yu-Shan Lin, James D. Baleja, David Baker, and Joshua A. Kritzer*

*corresponding author: joshua.kritzer@tufts.edu

Peptide Synthesis and Purification

Fmoc-protected amino acids were purchased from Anaspec, ChemPep and Novabiochem, except for (2*S*,4*R*)-Fmoc-S-trityl-4-mercaptoproline which was purchased from Iris Biotech (all four stereoisomers of S-trityl-protected, N-Fmoc-protected 4-mercaptoproline are currently commercially available). 1-[Bis(dimethylamino)methylene-1*H*-1,2,3-triazolo[4,5-*b*]pyridinium 3-oxid hexafluorophosphate (HATU) and hydroxybenzotriazole (HOBt), and benzotriazole-1-yl-oxy-tris-pyrrolidino-phosphonium hexafluorophosphate (PyBOP), and Rink amide resin were purchased from ChemPep. Rink resin and Wang resin pre-loaded with glutamic acid were purchased from Novabiochem. Dimethylformamide (DMF), *N,N*-diisopropylethylamine (DIPEA), acetic anhydride, trifluoroacetic acid (TFA), dichloromethane (DCM), triisopropylsilane (TIPS), 2,6-lutidine, ethanedithiol (EDT), and piperidine were purchased from Sigma-Aldrich. Dibromo-*ortho*-dimethylbenzene, dibromo-*meta*-dimethylbenzene, dibromo-*para*-dimethylbenzene, and allyl bromide were purchased from Sigma-Aldrich.

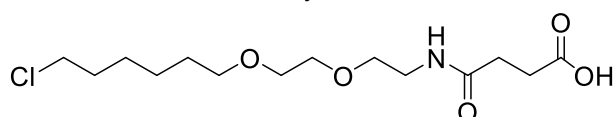
Linear peptides were synthesized on Rink Amide (0.8 mmol/g) or pre-loaded glutamate Wang resin (0.7 mmol/g) using standard Fmoc-chemistry and a Tribute automated synthesizer (Gyros Protein Technologies). For each coupling, 5 equivalents of HATU, 5 equivalents of HOBt, and 13 equivalents of DIPEA were dissolved in DMF, added and shaken with resin for 30 minutes at room temperature. Deprotection steps involves two 7-minute reactions with 20% piperidine in DMF. After final Fmoc deprotection, the N-terminal amine was acetylated by treatment with 5% (vol) acetic anhydride and 6% (vol) 2,6-lutidine in DMF for 30 minutes at room temperature. Alternatively, to cap the N-terminus with chloroalkane-carboxylic acid, 3 equivalents of chloroalkane-carboxylic acid (prepared as described),^{1,2} 3 equivalents of PyBOP, and 10 equivalents of DIPEA were dissolved in DMF and added to the resin for 1 hour at room temperature. The coupling efficiency was checked using a Kaiser test. Peptides were cleaved from the resin using cleavage cocktail (94% TFA, 2.5% EDT, 2.5% H₂O, and 1% TIPS) for 3-4 hours at room temperature. The resin was then filtered and the TFA solution was evaporated. The peptide was precipitated by adding cold diethyl ether (40 mL). After centrifugation and removal of ether, the pellet was dissolved in H₂O, frozen in liquid nitrogen, and lyophilized to remove solvent.

Peptide stapling by thiol bis-alkylation was performed essentially as described.^{3,4} Crude preparations of linear precursor was directly dissolved in 20 mL of 1:1 (vol/vol) acetonitrile:25 mM aqueous sodium bicarbonate at pH 8.0. The solution was then aliquoted into two new fractions (10 mL each) and were further diluted to 40 mL with 1:1 (vol/vol) acetonitrile:25 mM sodium bicarbonate pH 8.0. Bis-alkylation was carried out by adding 1.5 equivalents of α,α' -dibromo-*ortho*-dimethylbenzene, α,α' -dibromo-*meta*-dimethylbenzene, α,α' -dibromo-*para*-dimethylbenzene, or allyl bromide and reacting for 2 hours. Reactions were monitored by matrix assisted laser desorption/ionization (MALDI) mass spectrometry, and were complete within 1-2 hours. The reactions were then neutralized with TFA, frozen in liquid nitrogen, and lyophilized to remove solvent. Purification of the resulting peptides was achieved via high performance liquid chromatography (HPLC) on a reversed-phase C8 or C18 column. Analytical HPLC was used to verify >95% purity for all peptide preparations, and MALDI-MS was used to confirm the molecular weights for the expected peptides (Table S1).

Table S1. Peptide names, sequences, calculated masses, and observed masses.

Peptide	Sequence	N-term	C-term	Thiols attached to:	Calc. [M+H] ⁺	Obs. [M+Na] ⁺
ΔHP7	TWNPATGKWT	acetyl	amide	---	1209.47	1203.73
ΔHP7-GC-a	TWN 4 AT C KWT	acetyl	amide	allyl	1360.63	1354.19
ΔHP7-GC-o	TWN 4 AT C KWT	acetyl	amide	<i>ortho</i> -dimethyl benzene	1382.63	1406.03
ΔHP7-GC-m	TWN 4 AT C KWT	acetyl	amide	<i>meta</i> -dimethyl benzene	1382.63	1406.04
ΔHP7-GC-p	TWN 4 AT C KWT	acetyl	amide	<i>para</i> -dimethyl benzene	1382.63	1406.04
ΔHP7-KC-a	TWN 4 ATGCWT	acetyl	amide	allyl	1289.51	1312.29
ΔHP7-KC-o	TWN 4 ATGCWT	acetyl	amide	<i>ortho</i> -dimethyl benzene	1311.51	1334.34
ΔHP7-KC-m	TWN 4 ATGCWT	acetyl	amide	<i>meta</i> -dimethyl benzene	1311.51	1334.34
ΔHP7-KC-p	TWN 4 ATGCWT	acetyl	amide	<i>para</i> -dimethyl benzene	1311.51	1334.35
HP7	KTWNPATGKWTE	amine	acid	---	1418.70	1419.97
4MP-a	KTWyCTpXG4GWTE	amine	acid	allyl	1720.74	1720.74
4MP-m	KTWyCTpXG4GWTE	amine	acid	<i>meta</i> -dimethyl benzene	1742.73	1742.46
Δ4MP-a	TWYCTpXG4GWT	acetyl	amide	allyl	1504.63	1503.93
Δ4MP-m	TWYCTpXG4GWT	acetyl	amide	<i>meta</i> -dimethyl benzene	1526.62	1526.00
ct-HP7	KTWNPATGKWTE	chloro-alkane	acid	---	1722.85	1723.39
ct-ΔHP7	TWNPATGKWT	chloro-alkane	amide	---	1472.80	1471.45
ct-4MP-a	KTWyCTpXG4GWTE	chloro-alkane	acid	allyl	2024.90	2047.75 (+Na)
ct-4MP-m	KTWyCTpXG4GWTE	chloro-alkane	acid	<i>meta</i> -dimethyl benzene	2046.88	2048.58
ct-Δ4MP-a	TWYCTpXG4GWT	chloro-alkane	amide	allyl	1767.76	1767.68
ct-Δ4MP-m	TWYCTpXG4GWT	chloro-alkane	amide	<i>meta</i> -dimethyl benzene	1789.74	1788.91
4MP-a-p7G	KTWyCTGXG4GWTE	amine	acid	<i>allyl</i>	1680.92	1678.91
4MP-m-p7G	KTWyCTGXG4GWTE	amine	acid	<i>meta</i> -dimethyl benzene	1702.92	1701.38
4MP-a-X8G	KTWyCTpGG4GWTE	amine	acid	<i>allyl</i>	1694.94	1693.15
4MP-m-X8G	KTWyCTpGG4GWTE	amine	acid	<i>meta</i> -dimethyl benzene	1716.95	1714.68

4 denotes (2*S*,4*R*)-mercaptoproline, X denotes 1-aminocyclopropane-1-carboxylic acid, and lowercase letters denote D-amino acids. Chloroalkane-capped N-termini were acylated as described above using the chloroalkane-carboxylic acid **1**.



1

Design, Step 1. Screening for crosslinks with maximal compatibility with a target structural motif

Spatial coordinates for the target β -sheet motif were taken from a protein structure with a proline-containing antiparallel β -sheet (PDB: 1h2c, residues: 78 and 93).⁵ The motif (Figure S5, Step 1) was used as a template for building crosslinked motifs with different crosslinks. Then, we performed conformation generation using RDKit, where the backbone atoms of each crosslinked motif were the constrained atoms. Unconstrained conformations were also generated. We hypothesized that calculating the change in free energy between the constrained and unconstrained conformers would indicate the level of stabilization inherent in each specific crosslink. Thus, we sought crosslinks that maximized this difference for the β -sheet motif. As a second check on how compatible each crosslink was with the antiparallel strand, the constrained and unconstrained conformers were each randomly perturbed on their torsional degrees of freedom to yield slightly off-target decoy geometries. The goal of this step was to identify crosslinks that stabilize an alternative off-target geometry, which we hypothesized would make them less compatible with the target β -sheet motif.

A library of readily available crosslinks of various length was assembled. The full list of crosslinks are provided as SMILES strings in Table S2 and as chemical structures in Figure S1. A total of 10,000 conformers (2,500 constrained, constrained + perturbed, unconstrained, unconstrained + perturbed) were generated for each crosslink, and the conformers were minimized using AIMNet(SMD)-D4 without constraints. The Python script *run.py*, provided with this supplement, was used for these calculations. The final energies and conformations were recorded (Figure S5, Step 2).

To quantify the degree of stabilization, the ensemble of conformers and energies (examples shown in Figure S2) were analyzed via Boltzmann weighted probability of being near the desired state.⁶ This “folded-ness” metric was based on the backbone heavy atom RMSD to the template motif:

$$P_{Near} = \frac{\sum_i^N \exp\left(-\left(\frac{RMSD_i}{\lambda}\right)^2\right) * \exp\left(\frac{\Delta E_i}{-kT}\right)}{\sum_i^N \exp\left(\frac{\Delta E_i}{-kT}\right)}; \lambda = 1.0; kT = 0.59$$

The Python script *analyze.py*, provided with this supplement, was used for these calculations. P_{Near} values for all crosslinks are shown in Figure S4. Most of the crosslinks were fundamentally compatible with the target motif – all but the shortest crosslinks had at least one conformer with a backbone RMSD to the target motif of 1 Å or less. From the 40 crosslinks that were analyzed, 26 had P_{Near} values greater than 0.7, and no prominent torsion outliers in the lowest-energy state (example lowest-energy structures are shown in Figure S3). The crosslink denoted CMR (*meta*-dimethylbenzene linking a (2*S*,4*R*) 4-mercaptoproline to L-cysteine, where the 4-mercaptoproline is located somewhere N-terminal to the cysteine) was chosen as a representative crosslink that adequately fulfilled the target geometry. Many other crosslinks were predicted to fulfill the target geometry to a similar extent as crosslink CMR, and these crosslinks are being pursued in subsequent efforts. Eventually, it will be possible to correlate these calculations more broadly with experimentally observed effects on designed peptides.

Table S2. SMILES strings of staples used for conformational analysis

ID	SMILES
COS	<chem>CC(=O)N[C@H](C(=O)NC)CSCC1c(cccc1)CS[C@H](C1)C[C@@H](C(=O)NC)N1C(=O)C</chem>
CMS	<chem>CC(=O)N[C@H](C(=O)NC)CSCC1cc(ccc1)CS[C@H](C1)C[C@@H](C(=O)NC)N1C(=O)C</chem>
CPS	<chem>CC(=O)N[C@H](C(=O)NC)CSCC1ccc(cc1)CS[C@H](C1)C[C@@H](C(=O)NC)N1C(=O)C</chem>
CYS	<chem>CC(=O)N[C@H](C(=O)NC)CSCC1nc(ccc1)CS[C@H](C1)C[C@@H](C(=O)NC)N1C(=O)C</chem>
CSS	<chem>CC(=O)N[C@H](C(=O)NC)CSS[C@H](C1)C[C@@H](C(=O)NC)N1C(=O)C</chem>
C1S	<chem>CC(=O)N[C@H](C(=O)NC)CSCS[C@H](C1)C[C@@H](C(=O)NC)N1C(=O)C</chem>
C2S	<chem>CC(=O)N[C@H](C(=O)NC)CSCCS[C@H](C1)C[C@@H](C(=O)NC)N1C(=O)C</chem>
C3S	<chem>CC(=O)N[C@H](C(=O)NC)CSCCCS[C@H](C1)C[C@@H](C(=O)NC)N1C(=O)C</chem>
C4S	<chem>CC(=O)N[C@H](C(=O)NC)CSCCCCS[C@H](C1)C[C@@H](C(=O)NC)N1C(=O)C</chem>
CAS	<chem>CC(=O)N[C@H](C(=O)NC)CSCC=CCS[C@H](C1)C[C@@H](C(=O)NC)N1C(=O)C</chem>
COR	<chem>CC(=O)N[C@H](C(=O)NC)CSCC1c(cccc1)CS[C@@H](C1)C[C@@H](C(=O)NC)N1C(=O)C</chem>
CMR	<chem>CC(=O)N[C@H](C(=O)NC)CSCC1cc(ccc1)CS[C@@H](C1)C[C@@H](C(=O)NC)N1C(=O)C</chem>
CPR	<chem>CC(=O)N[C@H](C(=O)NC)CSCC1ccc(cc1)CS[C@@H](C1)C[C@@H](C(=O)NC)N1C(=O)C</chem>
CYR	<chem>CC(=O)N[C@H](C(=O)NC)CSCC1nc(ccc1)CS[C@@H](C1)C[C@@H](C(=O)NC)N1C(=O)C</chem>
CSR	<chem>CC(=O)N[C@H](C(=O)NC)CSS[C@@H](C1)C[C@@H](C(=O)NC)N1C(=O)C</chem>
C1R	<chem>CC(=O)N[C@H](C(=O)NC)CSCS[C@@H](C1)C[C@@H](C(=O)NC)N1C(=O)C</chem>
C2R	<chem>CC(=O)N[C@H](C(=O)NC)CSCCS[C@@H](C1)C[C@@H](C(=O)NC)N1C(=O)C</chem>
C3R	<chem>CC(=O)N[C@H](C(=O)NC)CSCCCS[C@@H](C1)C[C@@H](C(=O)NC)N1C(=O)C</chem>
C4R	<chem>CC(=O)N[C@H](C(=O)NC)CSCCCCS[C@@H](C1)C[C@@H](C(=O)NC)N1C(=O)C</chem>
CAR	<chem>CC(=O)N[C@H](C(=O)NC)CSCC=CCS[C@@H](C1)C[C@@H](C(=O)NC)N1C(=O)C</chem>
HOS	<chem>CC(=O)N[C@H](C(=O)NC)CCSC1c(cccc1)CS[C@H](C1)C[C@@H](C(=O)NC)N1C(=O)C</chem>
HMS	<chem>CC(=O)N[C@H](C(=O)NC)CCSC1cc(ccc1)CS[C@H](C1)C[C@@H](C(=O)NC)N1C(=O)C</chem>
HPS	<chem>CC(=O)N[C@H](C(=O)NC)CCSC1ccc(cc1)CS[C@H](C1)C[C@@H](C(=O)NC)N1C(=O)C</chem>
HYS	<chem>CC(=O)N[C@H](C(=O)NC)CCSC1nc(ccc1)CS[C@H](C1)C[C@@H](C(=O)NC)N1C(=O)C</chem>
HSS	<chem>CC(=O)N[C@H](C(=O)NC)CCSS[C@H](C1)C[C@@H](C(=O)NC)N1C(=O)C</chem>
H1S	<chem>CC(=O)N[C@H](C(=O)NC)CCSCS[C@H](C1)C[C@@H](C(=O)NC)N1C(=O)C</chem>
H2S	<chem>CC(=O)N[C@H](C(=O)NC)CCSCCS[C@H](C1)C[C@@H](C(=O)NC)N1C(=O)C</chem>
H3S	<chem>CC(=O)N[C@H](C(=O)NC)CCSCCCS[C@H](C1)C[C@@H](C(=O)NC)N1C(=O)C</chem>
H4S	<chem>CC(=O)N[C@H](C(=O)NC)CCSCCCCS[C@H](C1)C[C@@H](C(=O)NC)N1C(=O)C</chem>
HAS	<chem>CC(=O)N[C@H](C(=O)NC)CCSCC=CCS[C@H](C1)C[C@@H](C(=O)NC)N1C(=O)C</chem>
HOR	<chem>CC(=O)N[C@H](C(=O)NC)CCSC1c(cccc1)CS[C@@H](C1)C[C@@H](C(=O)NC)N1C(=O)C</chem>
HMR	<chem>CC(=O)N[C@H](C(=O)NC)CCSC1cc(ccc1)CS[C@@H](C1)C[C@@H](C(=O)NC)N1C(=O)C</chem>
HPR	<chem>CC(=O)N[C@H](C(=O)NC)CCSC1ccc(cc1)CS[C@@H](C1)C[C@@H](C(=O)NC)N1C(=O)C</chem>
HYR	<chem>CC(=O)N[C@H](C(=O)NC)CCSC1nc(ccc1)CS[C@@H](C1)C[C@@H](C(=O)NC)N1C(=O)C</chem>
HSR	<chem>CC(=O)N[C@H](C(=O)NC)CCSS[C@@H](C1)C[C@@H](C(=O)NC)N1C(=O)C</chem>
H1R	<chem>CC(=O)N[C@H](C(=O)NC)CCSCS[C@@H](C1)C[C@@H](C(=O)NC)N1C(=O)C</chem>
H2R	<chem>CC(=O)N[C@H](C(=O)NC)CCSCCS[C@@H](C1)C[C@@H](C(=O)NC)N1C(=O)C</chem>
H3R	<chem>CC(=O)N[C@H](C(=O)NC)CCSCCCS[C@@H](C1)C[C@@H](C(=O)NC)N1C(=O)C</chem>
H4R	<chem>CC(=O)N[C@H](C(=O)NC)CCSCCCCS[C@@H](C1)C[C@@H](C(=O)NC)N1C(=O)C</chem>
HAR	<chem>CC(=O)N[C@H](C(=O)NC)CCSCC=CCS[C@@H](C1)C[C@@H](C(=O)NC)N1C(=O)C</chem>

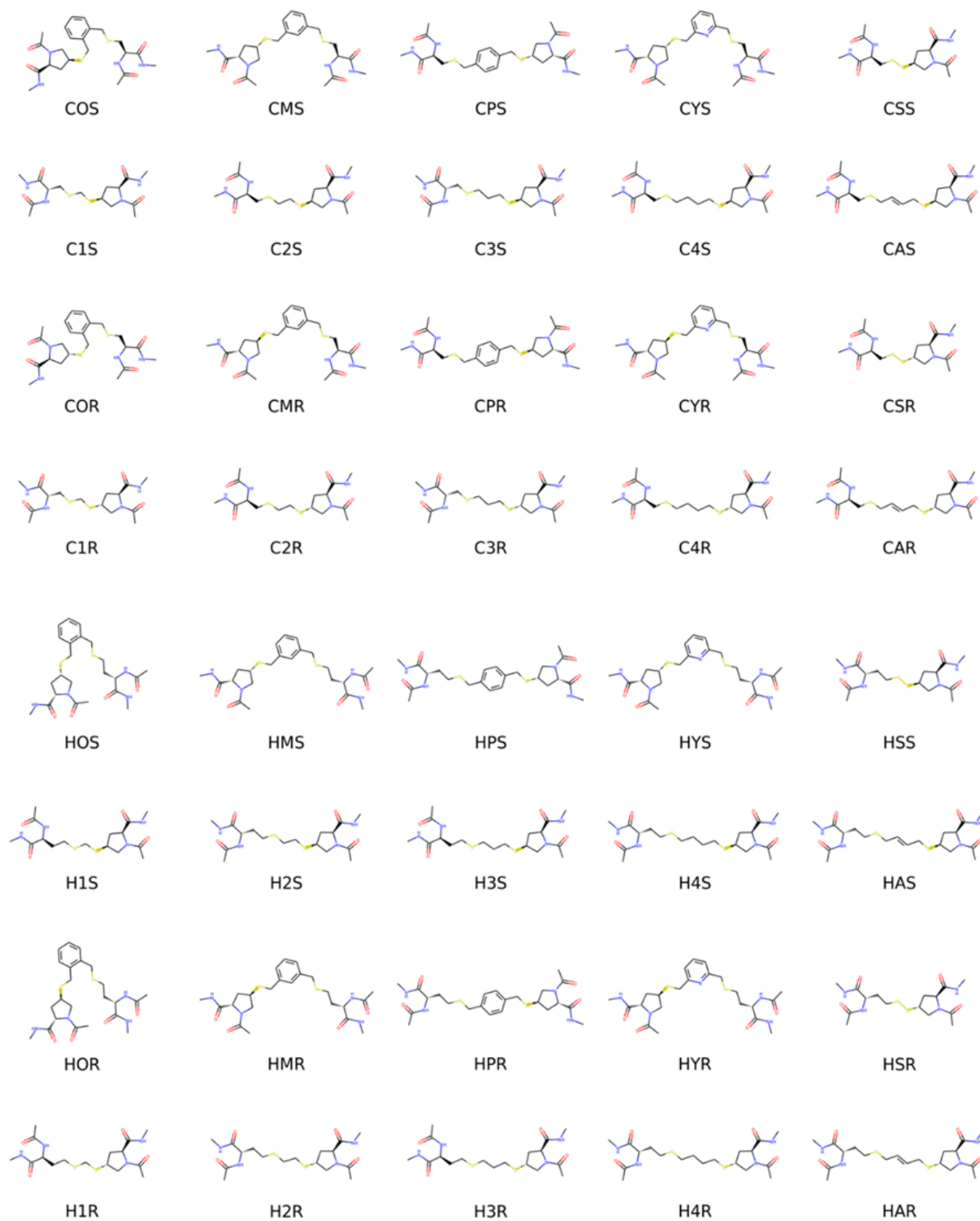


Figure S1. Chemical structures of staples used for conformational analysis

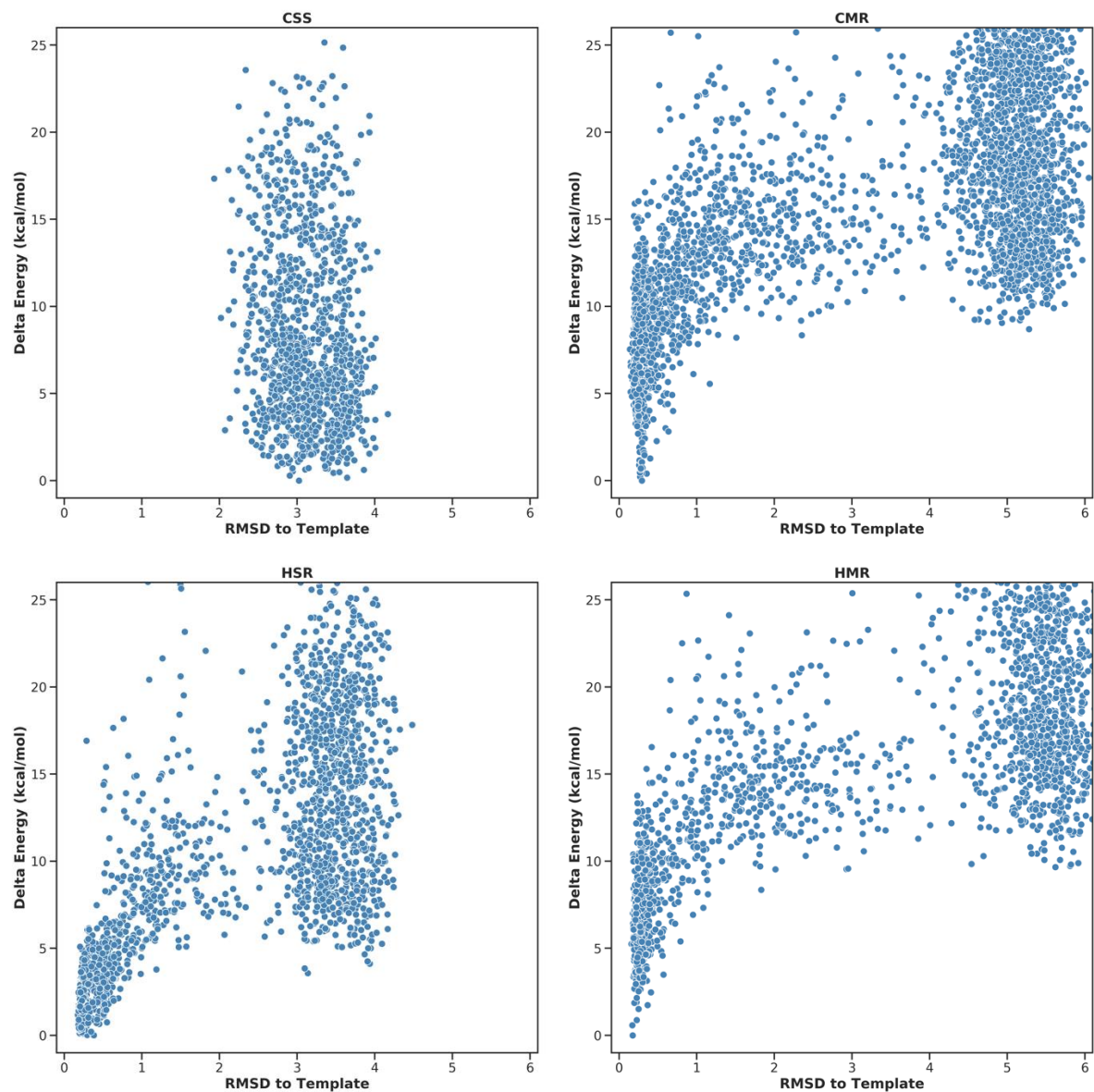


Figure S2. Conformational ensembles of selected staples.

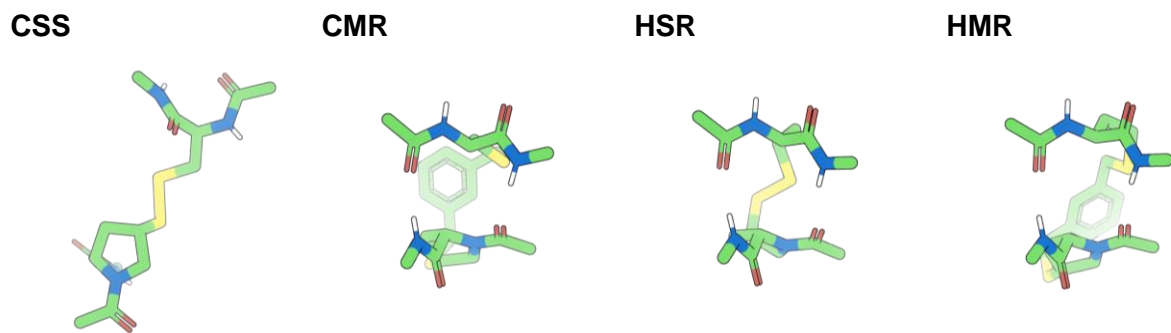


Figure S3. Lowest-energy conformations of selected staples.



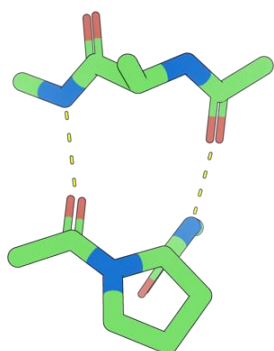
Figure S4. Folded-ness metric for all staples analyzed.

Design, Steps 2-4. Building a β -hairpin around the crosslinked antiparallel strand motif

Step 1 was to identify a maximally compatible crosslink for the antiparallel strand motif. Next, the CMR crosslink needed to be incorporated into a full β -hairpin. This was done in 3 additional steps. Step 2 was to graft a β -turn onto the stapled, antiparallel strands. To enable this grafting step, we first extended the stapled, antiparallel strands by one residue using an ideal β -sheet geometry. Then, the terminal residues were fused by aligning the plane of the terminal amide bonds with experimentally validated β -turns. As discussed in the main text, the optimal turn was identified as the D-Pro-Acpc turn described by Miller and colleagues (CSD entry 1412920).^{7,8} Lastly, sidechains were optimized in the context of the full peptide, including: D-Tyr to complement the 4MP on the opposite strand, beta-branched/aromatic residues to promote backbone torsions at β -strand positions, and glycine to avoid steric clashes. The final model was minimized using DFT (B3LYP/6-31G*(PCM)-D3) via Terachem^{18,19} (see supplemental script *input.min* and supplemental structure file *predict.pdb*). While several steps of this design process were not automated, current efforts are developing automated processes for β -hairpins and other structures based on the principles identified in this work.

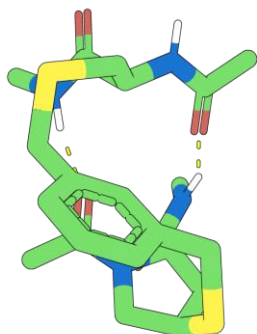
Figure S5. Schematic summary of computational design process.

Identify target structure (here, antiparallel kinked beta-strand)

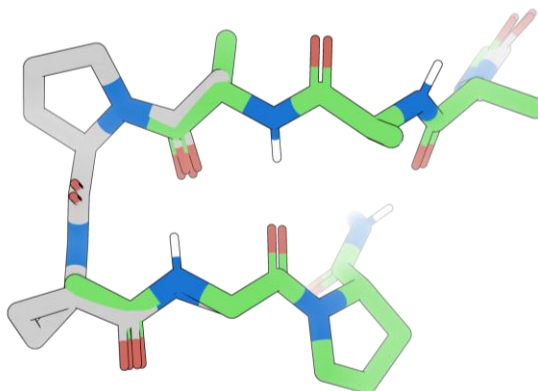


PDB: 1h2c

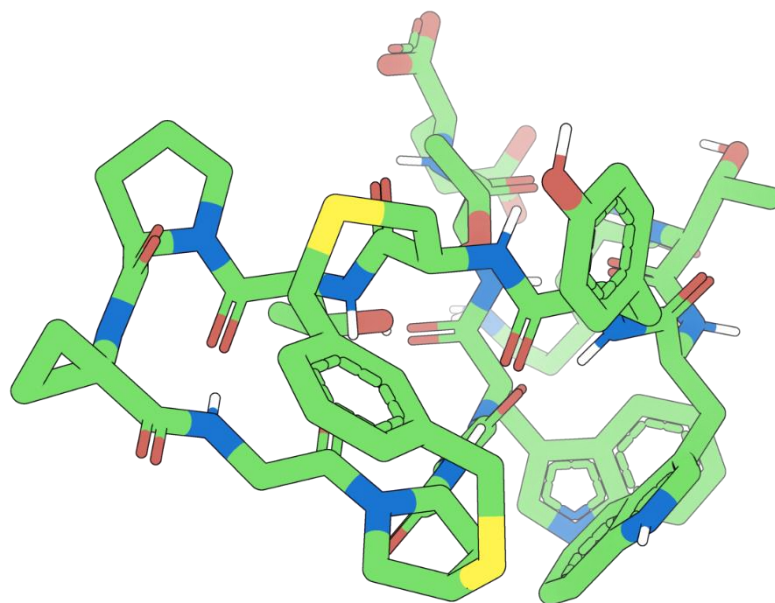
Step 1 – search for staples that are maximally compatible with the target structure using constrained conformer generation



Step 2 – align termini and fuse components using experimentally validated beta-turn motifs, isolating the best overall beta-hairpin structure



Steps 3,4 – optimize sidechains to promote designed backbone torsions



Additional Experimental Methods

Circular dichroism spectroscopy

Peptide concentrations for all circular dichroism (CD) spectroscopy measurements were calculated using A_{280} measurements on a Nanodrop-1000. CD spectra were acquired using a Jasco J-815 CD spectrometer at a concentration of 30 μ M in 10 mM KF (pH = 7.4) in a 0.1 cm pathlength cell.⁹ All CD was performed on three separate days with three separate sample preparations, and the three independent CD spectra were averaged to produce the final spectra shown. Thermal melts were performed by taking full CD spectra at 10 degree increments between 5 and 95 degrees Celsius.

Nuclear magnetic resonance spectroscopy

Peptides were dissolved in 90:10 H₂O:D₂O at concentrations between 1.0 and 3.0 mM. Higher concentration samples contained 4% DMSO-d₆. 1D and 2D ¹H NMR spectra were recorded at 288 K on a Bruker 600 MHz spectrometer equipped with a Prodigy Cryoprobe. **4MP-m** had a well-dispersed ¹H NMR spectrum, and chemical shifts were assigned with the help of TOCSY, NOESY, and ¹H-¹³C HSQC spectra (Fig. S10-S12, Table S5). 199 total NOEs were observed, of which 56 NOEs were between non-consecutive residues, including many potential cross-strand interactions (Fig. 3a and Table S6). Standard pulse programs from the Bruker library were used, with mixing times of 50.3 ms for the TOCSY and 200 ms for the NOESY. ¹H chemical shifts were referenced to DSS (δ 0.00 ppm) in water. Variable temperature experiments involved acquiring 1D and 2D ¹H spectra at 5 degree increments between 5 and 40 degrees Celsius.

Simulated annealing

We used a custom simulated annealing protocol because of the large number of artificial amino acids, the unusual staple, and the desire to faithfully simulate the constrained peptide in explicit water. The simulated annealing protocol began with building the chemical structure and energy minimizing it in vacuum. Next, beginning with the minimized structure, 100 replicas were generated with different initial velocities and each replica was annealed from 300 K to 800 K in vacuum for 200 ps in an NVT ensemble (300 K to 800 K in the first 100 ps, and then maintained at 800 K for 100 ps). After annealing, each replica was solvated in explicit water. The dimensions of the box were chosen such that the minimum distance between the walls of the box and any atom of the peptide was 1.0 nm. The entire system was then energy minimized using the steepest descent algorithm. Next, the system underwent a 500 ps NVT equilibration at 300 K. Lastly, the system was annealed from 300 K to 500 K and then subsequently down to 5 K over 1 ns in an NPT ensemble (the temperature increased from 300 K to 500 K in the first 100 ps, maintained at 500 K for 100 ps, decreased to 300 K in the following 500 ps, maintained at 300 K for 100 ps, and then decreased to 5 K in the last 200 ps). After all the simulation steps, the final structures from the 100 replicas were used for subsequent analysis.

The op1s2005 force field with tip4p water model was used for the simulations.^{10,11} Throughout the simulated annealing protocol, NOE-based distance restraints were applied to the peptide with a force constant of 1,000 kJ/mol/nm². The temperature was regulated using the v-rescale thermostat, with a coupling time constant of 0.1 ps.¹² The pressure was regulated using the Berendsen barostat, with a time coupling constant of 2.0 ps and isothermal compressibility of 4.5×10^{-5} bar⁻¹.¹³ The leapfrog algorithm with an integration time step of 2 fs was used to evolve the dynamics of the system.¹⁴ The LINCS algorithm was used to constrain all bonds containing

hydrogens to the equilibrium bond lengths.¹⁵ For the simulations in vacuum, the cutoffs of all non-bonded (electrostatics and van der Waals) interaction were set to 999.0 nm and the neighbor list was constructed once and kept constant thereafter. For the simulations in solvent, all non-bonded interactions as well as neighbor searching were truncated at 1.0 nm. Long-range electrostatics beyond the 1.0 nm were calculated using the particle mesh Ewald method with a Fourier spacing of 0.12 nm and an interpolation order of 4.^{16,17} To account for truncation of the Lennard-Jones interactions, a long-range analytic dispersion correction was applied to both energy and pressure.

Cell culture

HeLa cells for the stability assays were cultured in high-glucose DMEM with 10% fetal bovine serum and 1% penicillin/streptomycin. For the chloroalkane penetration assay, HeLa cells stably expressing HaloTag-GFP-mito (HGM)^{1,2,18} were cultured in high-glucose DMEM with 10% fetal bovine serum, 1% penicillin/streptomycin, and 1 μ g/mL puromycin. All cells were grown at 37 °C with 5% CO₂, and passaged every 2-3 days. As needed, HaloTag-expressing cells were selected with 20 μ g/mL puromycin in cell culture media.

Lysate stability assay

Prior to lysis, HeLa cells were trypsinized, washed in PBS, and pelleted. Cells were lysed with lysis buffer (50 mM Tris, 250 mM NaCl, 0.5% IGEPAL CA-630 detergent, pH 8.0) on ice for 15 min, then pelleted by centrifugation. Supernatants were collected, peptides were added to the lysate to a concentration of 150 μ M, and the peptides were incubated in lysate at 37 °C. Aliquots of 40 μ L were taken at each time point and enzymatic reactions were quenched using 160 μ L of ice-cold methanol. Samples were spun down for 10 min at 14,800 rpm in a table top centrifuge prior to analysis via reverse-phase analytical HPLC on a C18 column. Chromatogram peaks were integrated to measure amount remaining at each time point. Peak volumes for each timepoint were normalized to the zero hour timepoint area to determine percentage of peptide remaining. Data presented is the average of three biological replicates performed on different days, with error bars representing standard error of the mean. Predominant masses of degradation products were detected using MALDI-TOF mass spectrometry.

Chloroalkane penetration assay (CAPA)

CAPA was performed as described.^{1,2} HGM cells were seeded at a density of 4 x 10⁴ cells per well in a tissue culture treated 96-well plate to reach a confluency of 50-80% at the start of the experiment. Once the cells adhered, the cell culture media was replaced with optiMEM media. Serial dilutions of chloroalkane-tagged peptides (ct-peptides) were performed in sterile filtered water with 2.5 % DMSO, and added to the cells (final DMSO concentration was 0.5%). Samples were incubated at 37 °C for 4 hours, and then washed with fresh optiMEM for 15 mins. Cells were incubated at room temperature with 5 μ M chloroalkane-tagged tetramethylrhodamine (prepared as described)^{1,2} for 15 mins, then subsequently washed with optiMEM for 30 mins. Cells were trypsinized, resuspended in PBS, and analyzed by benchtop flow cytometry for red fluorescence (Guava EasyCyte, EMD Millipore). Data collection and analysis were performed as described.^{1,2}

Supplemental Results

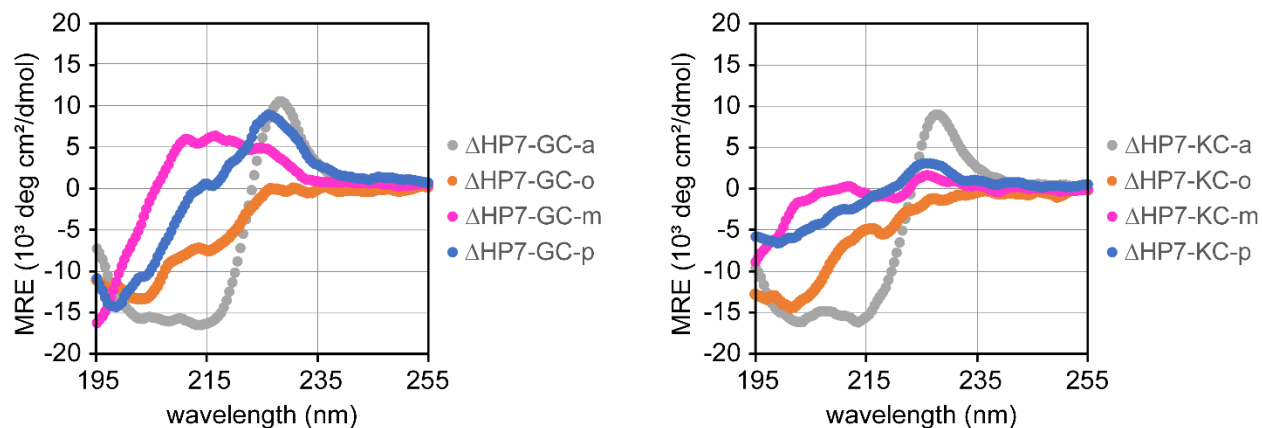


Figure S6. CD spectra for Δ HP7 analogs containing 4-mercaptoproline staples. Truncated hairpin Δ HP7 was substituted with a (2*S*,4*R*) 4-mercaptoproline for its proline, and a cysteine for either its glycine (Δ HP7-GC series) or its lysine (Δ HP7-KC series). These peptides were then stapled with either *ortho*, *meta*, or *para*-dibromomethylbenzene, or alkylated with allyl bromide to provide an unstapled control. None of these 4MP-containing, stapled analogs of Δ HP7 had greater β -hairpin structure than the parent peptide Δ HP7.

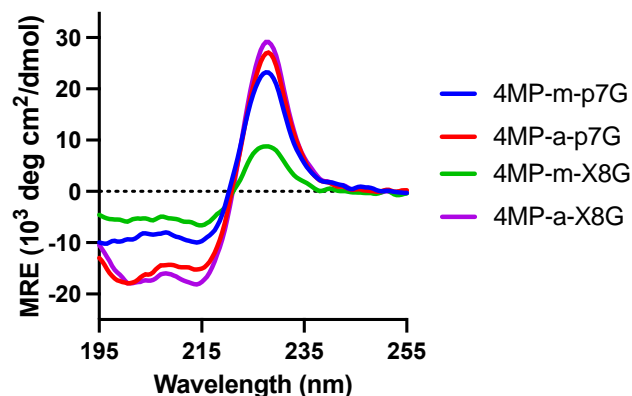


Figure S7. CD spectra for analogs p7G and X8G with modified beta-turns. Key residues responsible for the designed β -turn, D-proline and Acpc (X), were changed to glycine and then either stapled with *meta*-dibromomethylbenzene or alkylated with allyl bromide to provide an unstapled control. While all four peptides retained β -hairpin secondary structure, none were as structured as the parent 4MP-m. Both analogs also had less hairpin structure when stapled, in contrast to 4MP-m.

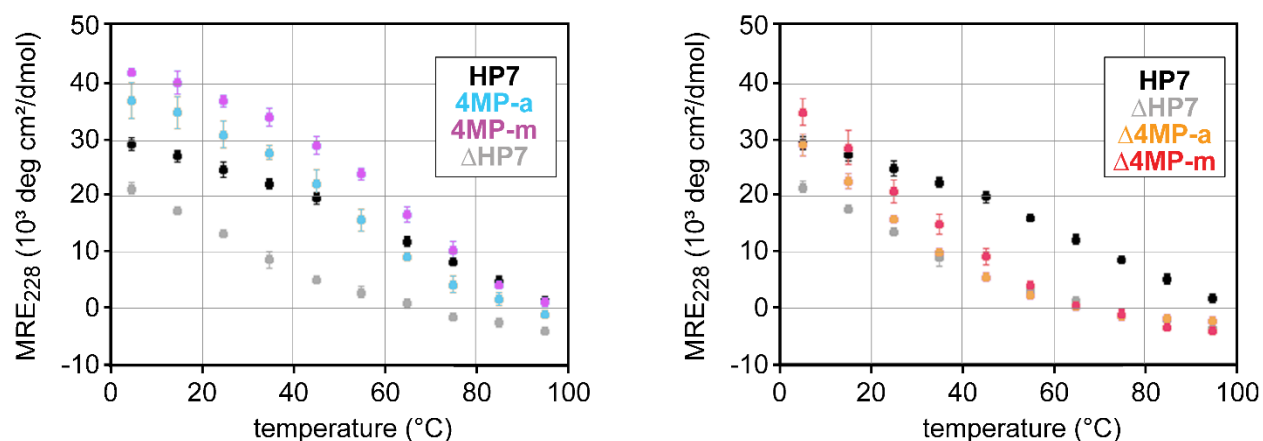


Figure S8. CD thermal melts for HP7, Δ HP7, and computationally designed, 4MP-stapled analogs. Error bars show standard errors of the mean from three independent trials.

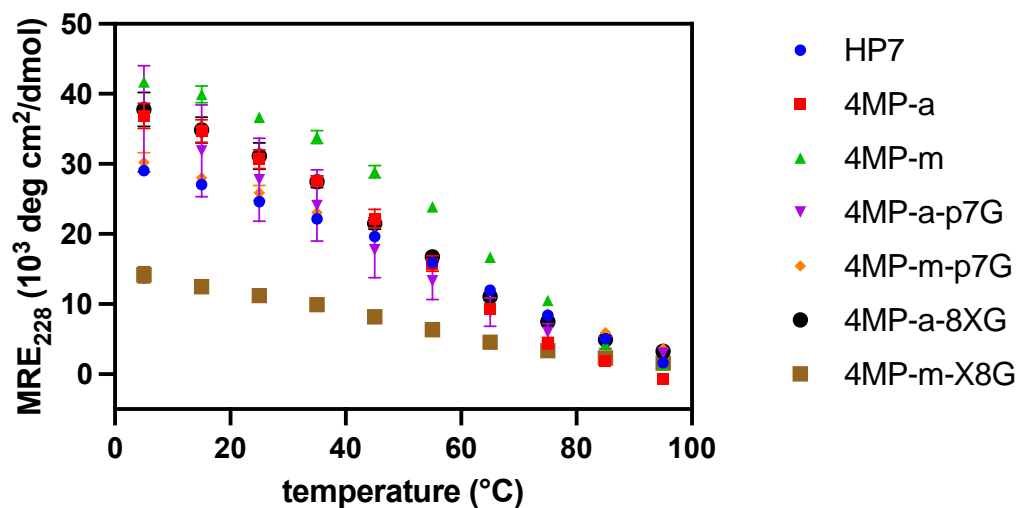


Figure S9. Thermal melts for analogs p7G and X8G with modified beta-turns. Error bars show standard errors of the mean from three independent trials.

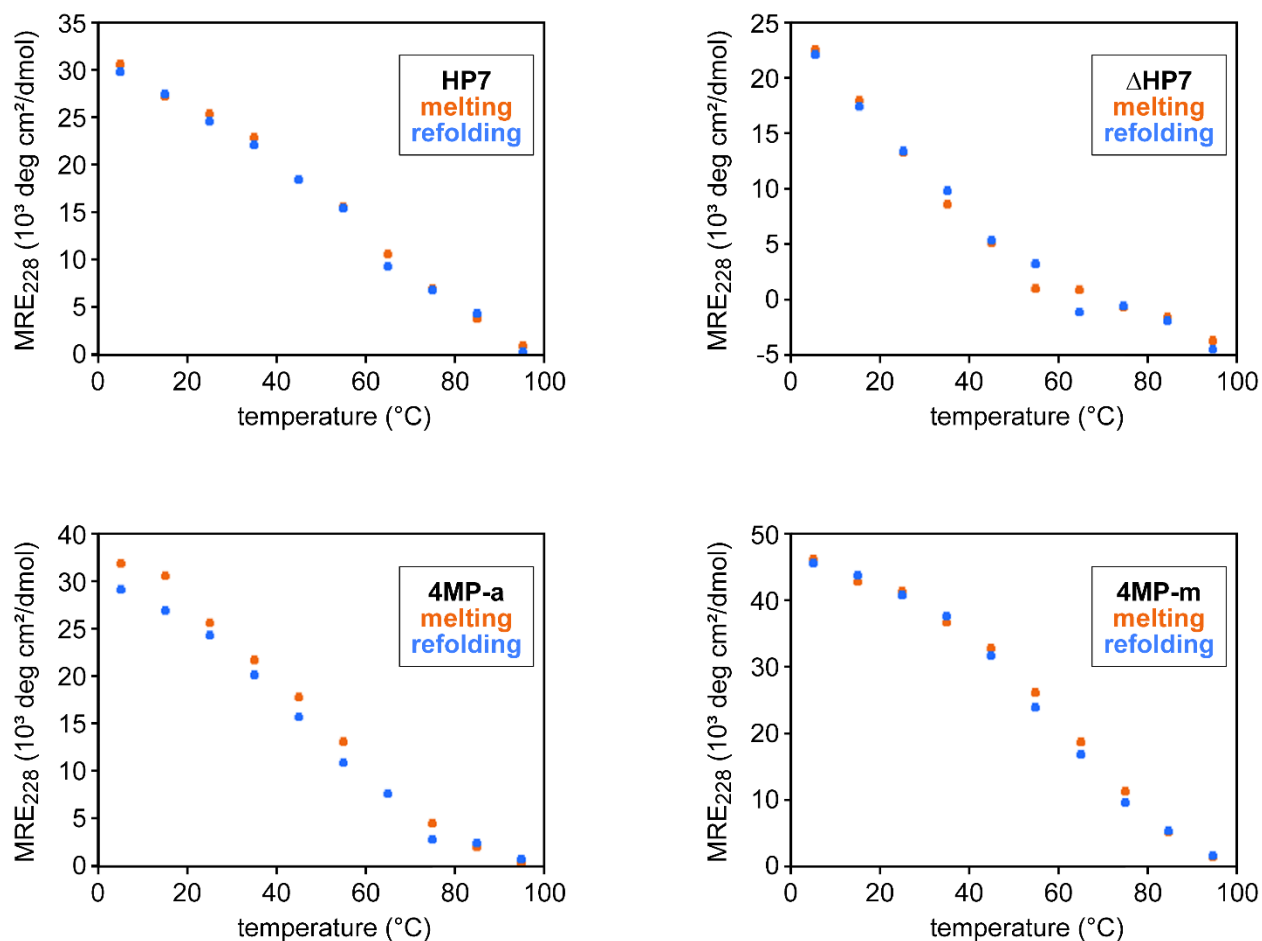


Figure S10. Thermal melt reversibility. Transitions measured during thermal melts were confirmed to be reversible unfolding by refolding after melting.

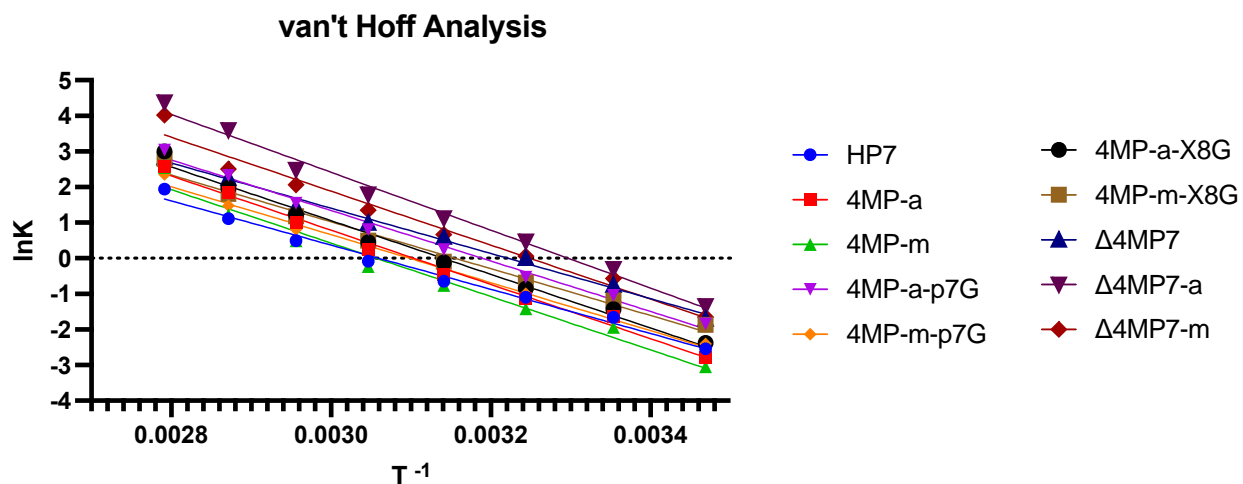


Figure S11. van't Hoff analysis of thermal unfolding data. Plots show $\ln K$ versus $1/T$ for controls **HP7** and **ΔHP7** , stapled hairpin peptides, and unstapled hairpin peptides. Slopes and intercepts from linear fits shown were used to calculate enthalpy and entropy values for thermal unfolding (Table S3).

Table S3. Summary of CD data and thermal unfolding thermodynamics for HP7, Δ HP7, and computationally designed, 4MP-stapled analogs. T_{50} values are calculated as the temperature at which the mean residue ellipticity near 228 nm was halfway between the starting value and the minimum observed value for Δ HP7 at 95 °C, which was used as the value indicating 100% unfolded structure. Errors are provided as standard errors of the mean from T_{50} values calculated from three independent thermal melt experiments.

Peptide	Mean Residue Ellipticity (MRE) at maximum near 228 nm at room temperature	T_{50} (°C)	Enthalpy (kJ/mol)	Entropy (J/mol)
HP7	26,900	58.7 ± 1.0	51.6	158
Δ HP7	16,600	31.9 ± 0.9	52.8	170
4MP-a	34,100	50.8 ± 0.6	63.4	197
4MP-m	38,000	58.5 ± 0.9	62.4	190
Δ 4MP-a	17,400	28.4 ± 0.1	67.6	223
Δ 4MP-m	23,500	32.1 ± 0.8	63.0	204
4MP-a-p7G	36,900	44.8 ± 1.2	58.9	170
4MP-m-p7G	23,000	56.7 ± 1.0	54.7	188
4MP-a-X8G	28,900	50.8 ± 1.2	61.3	167
4MP-m-X8G	8,700	51.0 ± 0.7	52.9	192

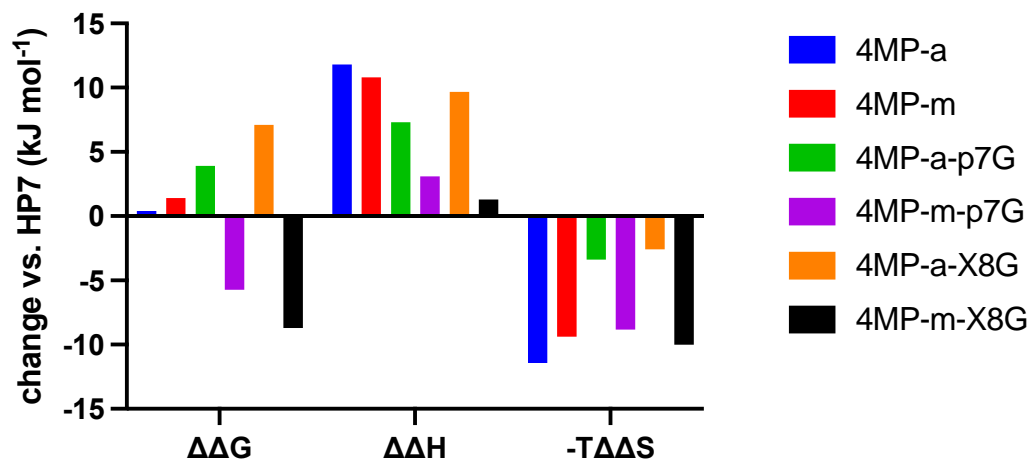


Figure S12. Summary of changes in thermodynamics of folding relative to HP7. The differences in free energy, enthalpy, and entropy obtained from a van't Hoff analysis (Figure S11, Table S3) for the stapled and unstapled hairpin peptides, relative to HP7.

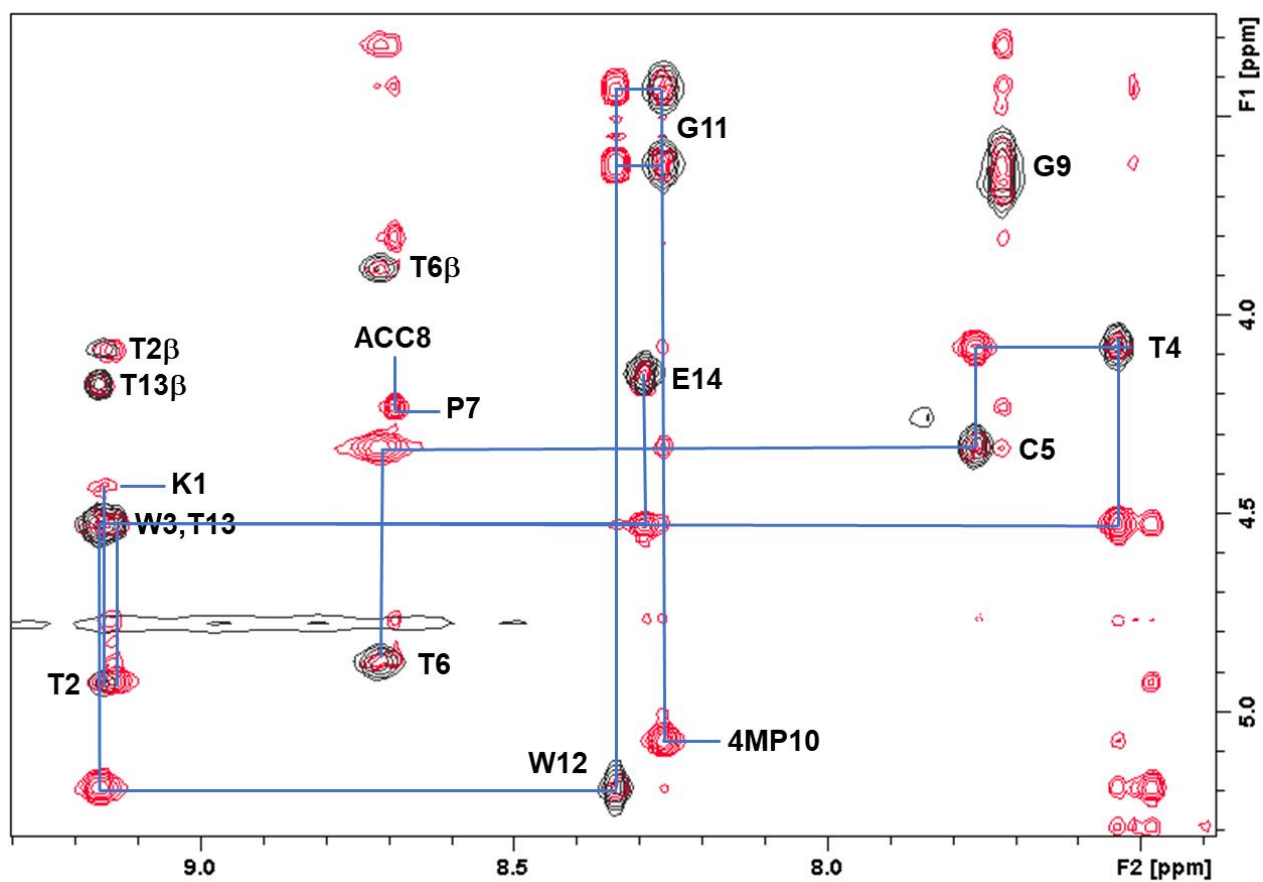


Figure S13. ^1H TOCSY/NOESY spectra for 4MP-m, “fingerprint” amide-to- $\text{H}\alpha$ region. The TOCSY spectrum is shown in black and the NOESY is shown in red. A “backbone walk” through cross-peaks is shown with blue lines.

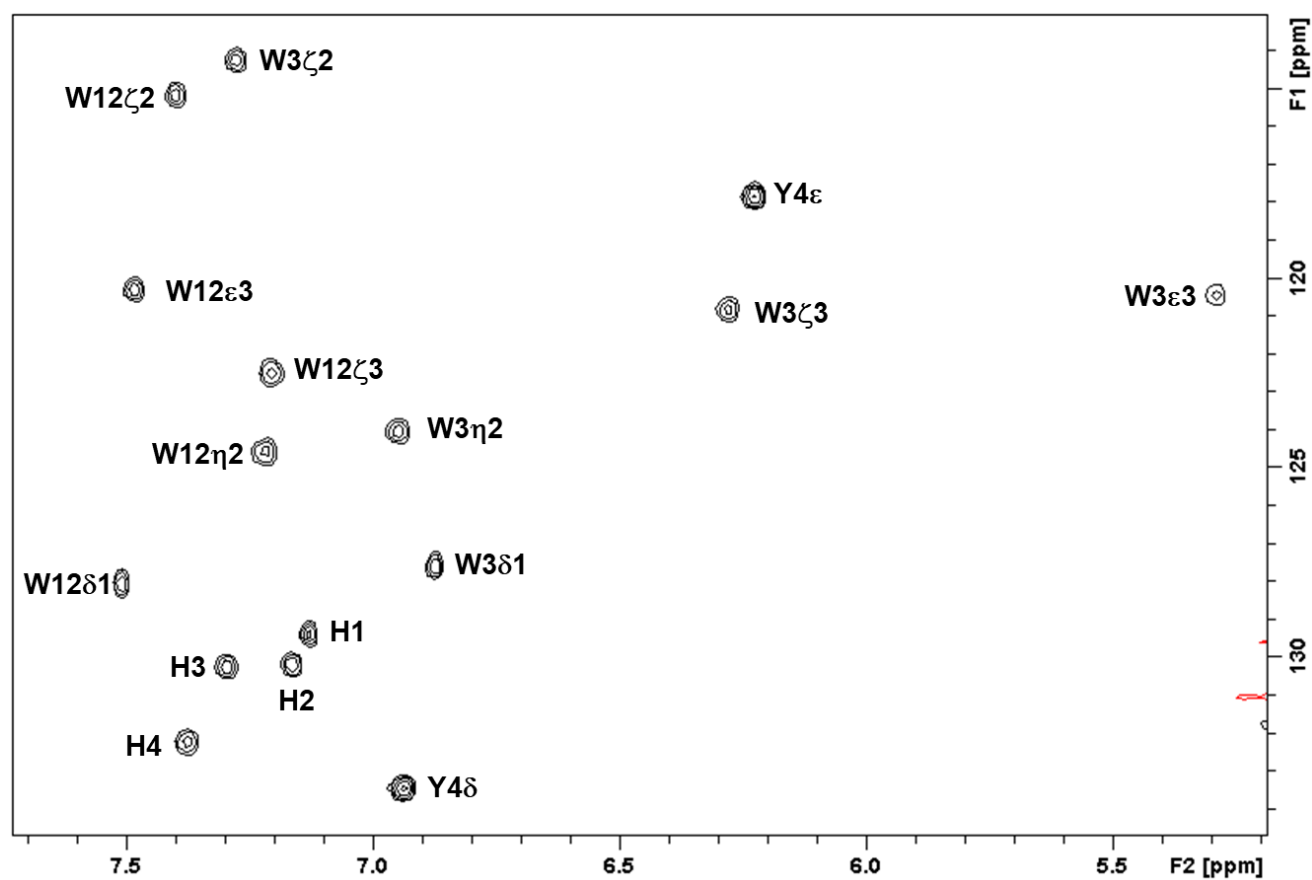


Figure S14. Aromatic HSQC spectrum for 4MP-m. H1-H4 refer to the aromatic protons and attached carbons for the *meta*-dibromobenzene linker.

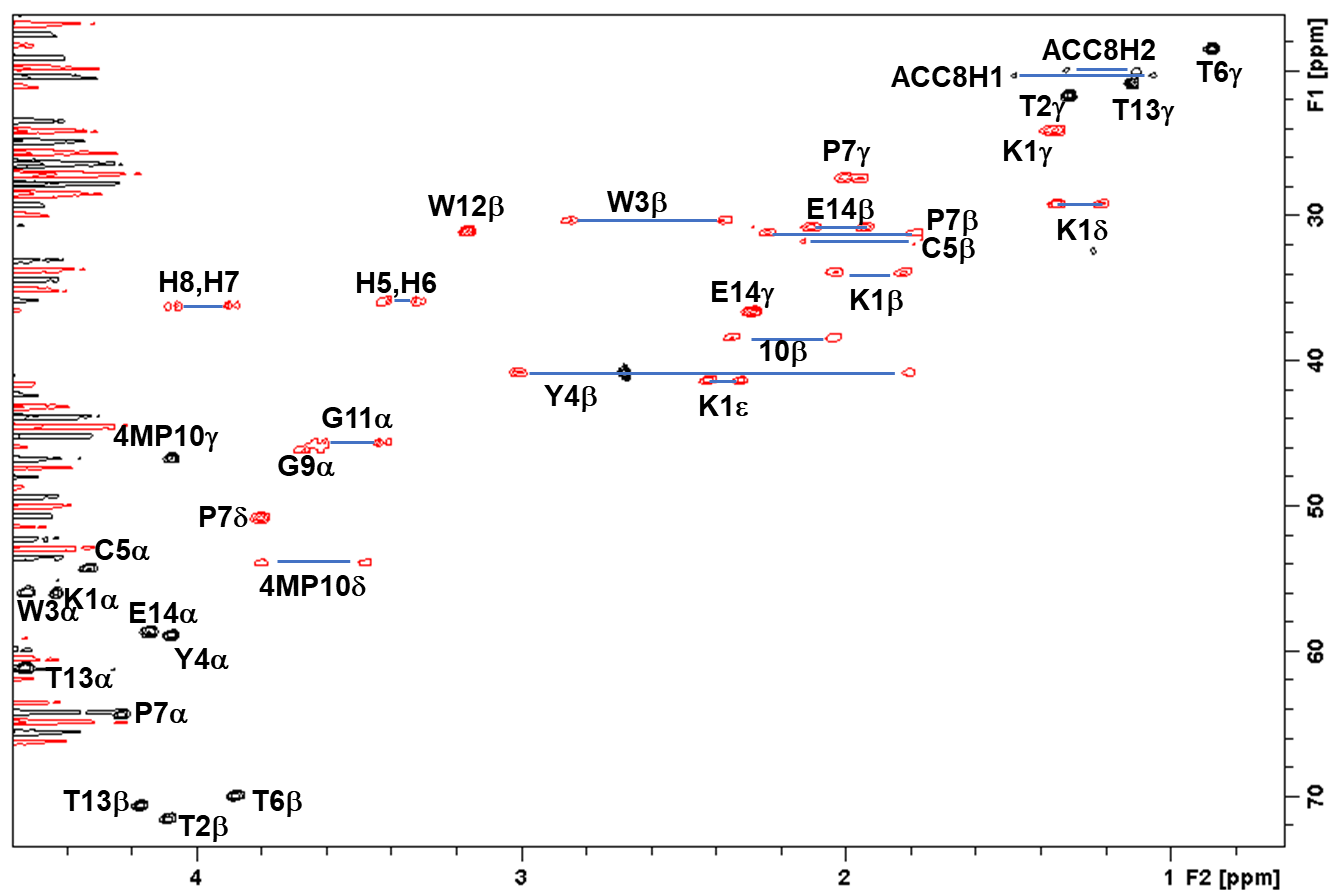


Figure S15. Aliphatic HSQC spectrum for 4MP-m. Correlations are highlighted with blue lines, with protons of methylene groups shown in red and other protons shown in black. H5-H8 refer to the aliphatic protons and attached carbons for the *meta*-dibromobenzene linker.

Table S4. Chemical shift assignments for 4MP-m. Proton chemical shifts that could be definitively assigned are listed, with associated carbon chemical shifts in parentheses.

Residue	NH	α H (α C)	β H, β H (β C)	Other H (other C)
Lys1	n/a	4.45 (55.9)	2.03, 1.818 (33.8)	γ : 1.362, 1.372 (24.06); δ : 1.356, 1.226 (29.11); ϵ : 2.322, 2.425 (41.3)
Thr2	9.17	4.94 (61.73)	4.09 (71.5)	1.31 (21.67)
Trp3	9.14	4.51 (55.92)	2.86, 2.40 (30.27)	ϵ 1 10.05; δ 1 6.88 (127.58); ϵ 3 5.26 (120.4); ζ 3 6.28 (120.8); η 2 6.95 (123.95); ζ 2 7.28 (114.21)
D-Tyr4	7.51	4.08 (58.9)	3.02, 1.80 (40.69)	δ : 6.94 (133.43), ϵ : 6.24 (117.81)
Cys5	7.76	4.33 (54.16)	2.14, 1.78 (31.7)	
Thr6	8.72	4.88	3.88 (69.93)	0.87 (18.41)
D-Pro7		4.23 (64.29)	2.23, 1.79 (31.3)	γ 2.01, 1.95 (27.3); δ 3.80, 3.77 (50.78)
ACPC8	8.70	n/a	H12: 1.48 (20.3); H21: 1.32 (19.9); H22: 1.11, (19.9); H11: 1.06 (20.3)	
Gly9	7.72	3.65, 3.60 (45.98)		
4MP10		5.06 (61.66)	2.34, 2.04 (38.2)	γ : 4.074 (46.65); δ 3.802, 3.476 (53.8)
Gly11	8.26	3.62, 3.43 (45.53)		
Trp12	8.34	5.19 (55.95)	3.16, 3.16 (31.04)	ϵ 1 10.36; δ 1 7.51 (128.02); ϵ 3 7.48 (120.25); ζ 3 7.21 (122.47); η 2 7.215 (124.5); ζ 2 7.395 (115.13)
Thr13	9.16	4.53 (61.09)	4.17 (70.59)	1.13 (20.78)
Glu14	8.30	4.15 (58.62)	2.11, 1.95 (30.67)	γ 2.29 (36.53)
<i>meta</i> -dibromo benzene (MX15)			H8 4.07; H7 3.891 (36.11); H5 3.421; H6 3.317 (35.8)	H1: 7.128 (129.3); H2: 7.163 (130.19); H3: 7.379 (132.2); H4: 7.294 (130.22)

Table S5. NOEs observed for 4MP-m.

Res1 ID	Res1 Name	H1 Name	Res2 ID	Res2 Name	H2 Name	Distance restraints from NMR (Å)	Percent of cluster 1 with lower-bound violation	Average lower-bound violation (Å)	Percent of cluster 1 with upper-bound violation	Average upper-bound violation (Å)
3	TRP	H	3	TRP	HB2	2.4 ~ 3.6	0	-	0	-
3	TRP	H	3	TRP	HB3	2.3 ~ 3.5	0	-	0	-
5	CYS	H	5	CYS	HA	3.0 ~ 4.4	100	0.089	0	-
5	CYS	H	5	CYS	HB3	2.2 ~ 3.4	0	-	0	-
5	CYS	H	5	CYS	HB2	2.4 ~ 3.6	91.7	0.079	0	-
4	DTYR	H	4	DTYR	HA	2.5 ~ 3.7	0	-	0	-
4	DTYR	H	4	DTYR	HB3	2.8 ~ 4.2	0	-	0	-
4	DTYR	H	4	DTYR	HB2	2.6 ~ 4.0	0	-	0	-
4	DTYR	HD#	4	DTYR	HB2	2.1 ~ 5.1	0	-	0	-
4	DTYR	HE#	5	CYS	HB2	2.6 ~ 6.0	0	-	0	-
9	GLY	H	9	GLY	HA3	2.4 ~ 3.6	8.3	-	0	-
9	GLY	H	9	GLY	HA2	2.5 ~ 3.7	0	-	0	-
11	GLY	H	11	GLY	HA2	2.6 ~ 4.0	0	-	0	-
12	TRP	H	12	TRP	HB#	2.0 ~ 3.0	0	-	0	-
12	TRP	H	12	TRP	HA	2.6 ~ 4.0	0	-	0	-
6	THR	H	6	THR	HA	2.9 ~ 4.3	83.3	0.011	0	-
6	THR	H	6	THR	HB	3.1 ~ 4.7	0	-	0	-
6	THR	H	6	THR	HG2#	2.6 ~ 5.0	0	-	0	-
15	MXY	H1	5	CYS	HA	2.2 ~ 3.4	0	-	0	-
8	ACPC	H	7	DPRO	HA	2.2 ~ 3.2	0	-	100	-0.367
12	TRP	HE1	12	TRP	HZ2	2.5 ~ 3.7	0	-	0	-
12	TRP	HH2	12	TRP	HZ2	1.8 ~ 2.8	0	-	0	-
12	TRP	HE1	12	TRP	HH2	3.5 ~ 5.3	0	-	0	-
12	TRP	HZ3	2	THR	HA	2.7 ~ 4.1	8.3	-	0	-
3	TRP	HE1	3	TRP	HD1	2.0 ~ 3.0	0	-	0	-
3	TRP	HE1	3	TRP	HZ2	2.3 ~ 3.5	0	-	0	-
3	TRP	HH2	3	TRP	HZ3	2.2 ~ 3.4	0	-	0	-
3	TRP	HZ2	3	TRP	HZ3	2.8 ~ 4.2	0	-	100	-0.106
15	MXY	H1	10	4MP	HA	2.4 ~ 3.6	0	-	0	-
11	GLY	H	10	4MP	HA	1.8 ~ 2.8	0	-	0	-
8	ACPC	H	8	ACPC	H12	2.9 ~ 4.3	0	-	0	-
8	ACPC	H	8	ACPC	H21	2.7 ~ 4.1	0	-	100	-0.066
8	ACPC	H	7	DPRO	HB3	2.6 ~ 4.0	0	-	0	-
8	ACPC	H	8	ACPC	H22	2.2 ~ 3.4	0	-	33.3	-
8	ACPC	H	8	ACPC	H11	2.3 ~ 3.5	0	-	0	-
11	GLY	HA3	6	THR	HG2#	3.3 ~ 5.9	66.7	-	0	-

8	ACPC	H	7	DPRO	HG3	3.0 ~ 4.4	33.3	-	8.3	-
8	ACPC	H	7	DPRO	HB2	3.2 ~ 4.8	0	-	0	-
8	ACPC	H	15	MXY	H5	3.2 ~ 4.8	0	-	0	-
8	ACPC	H	7	DPRO	HD#	2.6 ~ 3.8	0	-	0	-
3	TRP	HE1	10	4MP	HB3	2.6 ~ 4.0	33.3	-	0	-
3	TRP	HE1	10	4MP	HB2	3.2 ~ 4.8	0	-	0	-
3	TRP	HE1	4	DTYR	HB3	3.2 ~ 4.8	0	-	0	-
3	TRP	HE1	3	TRP	HB3	3.6 ~ 5.4	0	-	0	-
3	TRP	HE1	3	TRP	HH2	3.2 ~ 4.8	0	-	100	-0.274
9	GLY	H	8	ACPC	H21	3.5 ~ 5.3	0	-	0	-
9	GLY	H	8	ACPC	H12	3.7 ~ 5.5	0	-	0	-
9	GLY	H	8	ACPC	H22	3.4 ~ 5.2	0	-	0	-
9	GLY	H	8	ACPC	H11	3.5 ~ 5.3	0	-	0	-
15	MXY	H5	8	ACPC	H22	3.8 ~ 5.8	0	-	0	-
15	MXY	H6	8	ACPC	H22	4.0 ~ 6.0	0	-	33.3	-
15	MXY	H5	8	ACPC	H21	3.4 ~ 5.2	0	-	8.3	-
15	MXY	H6	8	ACPC	H21	3.5 ~ 5.3	0	-	91.7	-0.245
12	TRP	HE3	12	TRP	HB3	2.2 ~ 3.4	0	-	0	-
3	TRP	HD1	3	TRP	HB3	2.2 ~ 3.4	0	-	0	-
3	TRP	HD1	3	TRP	HB2	2.6 ~ 4.0	0	-	0	-
3	TRP	HD1	4	DTYR	HB3	2.4 ~ 3.6	33.3	-	0	-
5	CYS	H	4	DTYR	HB3	3.4 ~ 5.0	0	-	0	-
12	TRP	HD1	12	TRP	HB2	2.2 ~ 3.2	0	-	0	-
12	TRP	HA	12	TRP	HB2	2.6 ~ 4.0	0	-	0	-
3	TRP	HE3	3	TRP	HB2	3.3 ~ 4.9	100	0.425	0	-
4	DTYR	HE#	4	DTYR	HB3	3.5 ~ 7.3	0	-	0	-
12	TRP	HE1	12	TRP	H	4.0 ~ 6.0	0	-	0	-
3	TRP	HE1	11	GLY	H	4.0 ~ 6.0	0	-	0	-
3	TRP	HE1	4	DTYR	H	3.9 ~ 5.9	0	-	0	-
13	THR	H	13	THR	HG2#	2.6 ~ 5.0	0	-	0	-
14	GLU	H	13	THR	HG2#	2.8 ~ 5.2	0	-	0	-
12	TRP	H	6	THR	HG2#	2.9 ~ 5.3	0	-	0	-
11	GLY	H	6	THR	HG2#	2.8 ~ 5.2	0	-	0	-
11	GLY	H	4	DTYR	HB2	3.3 ~ 4.9	0	-	0	-
11	GLY	H	10	4MP	HB3	2.8 ~ 4.2	0	-	0	-
11	GLY	H	10	4MP	HB2	3.1 ~ 4.7	0	-	0	-
11	GLY	H	4	DTYR	H	2.3 ~ 3.5	0	-	0	-
11	GLY	H	15	MXY	H1	3.6 ~ 5.4	0	-	41.7	-
12	TRP	H	12	TRP	HD1	2.6 ~ 4.0	0	-	0	-
12	TRP	H	3	TRP	HZ3	3.2 ~ 4.8	8.3	-	0	-
12	TRP	H	11	GLY	HA3	2.2 ~ 3.4	0	-	0	-

12	TRP	H	11	GLY	HA2	2.2 ~ 3.4	0	-	0	-
6	THR	H	5	CYS	HA	2.2 ~ 3.4	25	-	0	-
11	GLY	H	5	CYS	HA	2.9 ~ 4.3	0	-	0	-
5	CYS	H	4	DTYR	HD#	2.9 ~ 6.3	0	-	0	-
5	CYS	H	4	DTYR	HE#	3.7 ~ 7.5	0	-	0	-
9	GLY	H	8	ACPC	H	2.2 ~ 3.4	0	-	0	-
6	THR	H	15	MXY	H1	3.7 ~ 5.5	0	-	0	-
8	ACPC	H	15	MXY	H1	3.8 ~ 5.6	0	-	100	-0.391
6	THR	H	10	4MP	HA	3.6 ~ 5.4	8.3	-	0	-
8	ACPC	H	6	THR	HA	2.8 ~ 4.2	0	-	0	-
8	ACPC	H	9	GLY	HA3	3.6 ~ 5.4	0	-	16.7	-
6	THR	H	15	MXY	H5	3.5 ~ 5.3	0	-	0	-
6	THR	H	15	MXY	H6	2.8 ~ 4.2	0	-	0	-
8	ACPC	H	7	DPRO	HG2	3.4 ~ 5.0	0	-	0	-
3	TRP	H	2	THR	HG2#	2.7 ~ 5.1	0	-	0	-
3	TRP	H	2	THR	HA	2.0 ~ 3.0	0	-	0	-
3	TRP	H	12	TRP	HZ3	2.8 ~ 4.2	8.3	-	0	-
5	CYS	H	13	THR	HG2#	3.2 ~ 5.8	0	-	75	-0.571
4	DTYR	H	13	THR	HG2#	3.3 ~ 5.9	0	-	16.7	-
4	DTYR	H	6	THR	HG2#	3.6 ~ 6.4	0	-	0	-
9	GLY	H	6	THR	HG2#	3.3 ~ 5.9	0	-	0	-
12	TRP	HE1	3	TRP	HZ3	2.8 ~ 4.2	16.7	-	0	-
12	TRP	HE1	3	TRP	HE3	3.5 ~ 5.3	33.3	-	0	-
12	TRP	HE1	12	TRP	HB#	3.5 ~ 5.3	0	-	0	-
3	TRP	HE1	10	4MP	HA	3.8 ~ 5.6	0	-	0	-
13	THR	H	12	TRP	H	3.5 ~ 5.3	0	-	0	-
13	THR	H	14	GLU	H	3.2 ~ 4.8	0	-	0	-
11	GLY	H	6	THR	H	3.3 ~ 4.9	0	-	0	-
13	THR	H	12	TRP	HE3	2.9 ~ 4.3	0	-	0	-
3	TRP	H	3	TRP	HD1	3.6 ~ 5.4	0	-	0	-
13	THR	H	12	TRP	HA	2.0 ~ 3.0	0	-	0	-
13	THR	H	13	THR	HB	2.7 ~ 4.1	16.7	-	0	-
3	TRP	H	2	THR	HB	2.7 ~ 4.1	0	-	58.3	-
13	THR	H	12	TRP	HB#	2.6 ~ 3.8	0	-	0	-
13	THR	H	1	LYS	HB2	3.7 ~ 5.5	41.7	-	0	-
14	GLU	H	14	GLU	HB3	2.6 ~ 3.8	8.3	-	16.7	-
14	GLU	H	14	GLU	HB2	3.0 ~ 4.6	41.7	-	0	-
14	GLU	H	14	GLU	HG#	3.2 ~ 4.8	0	-	0	-
9	GLY	H	15	MXY	H6	2.7 ~ 4.1	41.7	-	0	-
9	GLY	H	15	MXY	H5	3.0 ~ 4.6	0	-	8.3	-
9	GLY	H	10	4MP	HD3	3.3 ~ 4.9	0	-	16.7	-

9	GLY	H	10	4MP	HD2	3.4 ~ 5.0	0	-	100	-0.096
5	CYS	H	4	DTYR	HA	2.0 ~ 3.0	0	-	0	-
11	GLY	H	4	DTYR	HA	3.4 ~ 5.0	0	-	0	-
14	GLU	H	14	GLU	HA	2.3 ~ 3.5	16.7	-	0	-
9	GLY	H	7	DPRO	HA	3.2 ~ 4.8	0	-	0	-
14	GLU	H	13	THR	HA	2.0 ~ 3.0	0	-	0	-
5	CYS	H	4	DTYR	H	3.2 ~ 4.8	0	-	0	-
6	THR	H	9	GLY	H	2.7 ~ 4.1	0	-	0	-
12	TRP	HE1	12	TRP	HD1	2.1 ~ 3.1	0	-	0	-
12	TRP	HD1	3	TRP	HZ3	2.7 ~ 4.1	8.3	-	0	-
12	TRP	HZ2	3	TRP	HZ3	3.6 ~ 5.4	0	-	0	-
15	MXY	H3	4	DTYR	HE#	3.4 ~ 7.2	8.3	-	0	-
15	MXY	H2	4	DTYR	HE#	3.4 ~ 7.2	0	-	0	-
15	MXY	H1	4	DTYR	HE#	2.8 ~ 6.2	0	-	0	-
4	DTYR	H	10	4MP	HA	3.3 ~ 4.9	0	-	0	-
4	DTYR	H	12	TRP	HA	3.0 ~ 4.4	0	-	0	-
4	DTYR	H	3	TRP	HE3	3.2 ~ 4.8	0	-	0	-
12	TRP	HE3	12	TRP	HA	2.2 ~ 3.4	0	-	0	-
12	TRP	HE3	3	TRP	HE3	3.1 ~ 4.7	0	-	0	-
12	TRP	HE3	2	THR	HA	3.0 ~ 4.4	0	-	0	-
4	DTYR	H	3	TRP	HA	1.9 ~ 2.9	0	-	0	-
9	GLY	H	5	CYS	HA	3.2 ~ 4.8	0	-	25	-
15	MXY	H4	15	MXY	H8	2.4 ~ 3.6	83.3	0.033	0	-
15	MXY	H1	15	MXY	H8	2.5 ~ 3.7	0	-	100	-0.112
15	MXY	H4	15	MXY	H7	2.6 ~ 3.8	0	-	0	-
15	MXY	H3	15	MXY	H7	3.6 ~ 5.4	0	-	0	-
15	MXY	H1	15	MXY	H7	2.6 ~ 3.8	0	-	0	-
15	MXY	H1	10	4MP	HD2	3.0 ~ 4.4	0	-	0	-
12	TRP	HD1	11	GLY	HA3	3.4 ~ 5.2	0	-	75	-0.086
12	TRP	HD1	11	GLY	HA2	3.3 ~ 4.9	0	-	0	-
15	MXY	H1	9	GLY	HA3	2.7 ~ 4.1	0	-	83.3	-0.142
15	MXY	H4	10	4MP	HD3	3.2 ~ 4.8	0	-	100	-0.231
15	MXY	H1	10	4MP	HD3	2.4 ~ 3.6	100	0.192	0	-
15	MXY	H1	15	MXY	H5	2.6 ~ 3.8	0	-	0	-
15	MXY	H2	15	MXY	H5	2.4 ~ 3.6	0	-	0	-
15	MXY	H2	15	MXY	H6	2.8 ~ 4.2	0	-	0	-
12	TRP	HZ3	12	TRP	HB#	3.4 ~ 5.0	0	-	100	-0.246
12	TRP	HH2	3	TRP	HB3	3.1 ~ 4.7	0	-	58.3	-0.015
4	DTYR	H	3	TRP	HB3	3.2 ~ 4.8	0	-	0	-
4	DTYR	H	3	TRP	HB2	3.1 ~ 4.7	0	-	0	-
12	TRP	HE3	3	TRP	HB2	3.0 ~ 4.6	0	-	0	-

12	TRP	HE3	1	LYS	HB2	2.8 ~ 4.2	58.3	0.003	0	-
3	TRP	HZ2	10	4MP	HB2	2.6 ~ 3.8	58.3	0.02	0	-
12	TRP	HZ3	3	TRP	HB2	2.6 ~ 3.8	0	-	0	-
12	TRP	HZ3	1	LYS	HB2	3.4 ~ 5.2	0	-	0	-
15	MXY	H2	5	CYS	HB2	3.3 ~ 4.9	0	-	0	-
15	MXY	H2	5	CYS	HB3	3.7 ~ 5.5	83.3	0.164	0	-
15	MXY	H1	5	CYS	HB3	3.1 ~ 4.7	0	-	0	-
12	TRP	HE3	1	LYS	HD2	2.8 ~ 4.2	0	-	8.3	-
12	TRP	HE3	1	LYS	HD3	3.4 ~ 5.2	0	-	0	-
12	TRP	HZ3	1	LYS	HG2	3.0 ~ 4.6	0	-	33.3	-
3	TRP	HD1	4	DTYR	HB2	2.6 ~ 3.8	0	-	0	-
4	DTYR	HE#	5	CYS	HB3	3.2 ~ 6.8	0	-	0	-
3	TRP	HZ3	11	GLY	HA2	2.6 ~ 3.8	8.3	-	0	-
3	TRP	HZ3	11	GLY	HA3	3.3 ~ 4.9	0	-	0	-
4	DTYR	HE#	15	MXY	H7	3.5 ~ 7.3	0	-	0	-
4	DTYR	HE#	4	DTYR	HA	2.8 ~ 6.2	0	-	0	-
4	DTYR	HE#	5	CYS	HA	3.6 ~ 7.4	0	-	0	-
3	TRP	HE3	3	TRP	HZ3	2.2 ~ 3.4	0	-	0	-
3	TRP	HE3	3	TRP	HA	3.1 ~ 4.7	91.7	0.207	0	-
15	MXY	H6	5	CYS	HA	2.6 ~ 3.8	100	0.144	0	-
10	4MP	HG3	10	4MP	HD3	2.5 ~ 3.7	0	-	0	-
3	TRP	HA	3	TRP	HB3	3.0 ~ 4.4	0	-	0	-
6	THR	HB	13	THR	HG2#	3.1 ~ 5.7	0	-	0	-
7	DPRO	HD#	7	DPRO	HB3	2.9 ~ 4.3	0	-	0	-
15	MXY	H5	5	CYS	HB2	3.3 ~ 4.9	0	-	0	-
15	MXY	H5	5	CYS	HB3	3.2 ~ 4.8	0	-	0	-
15	MXY	H6	5	CYS	HB3	3.4 ~ 5.0	66.7	0.022	0	-
15	MXY	H6	5	CYS	HB2	3.4 ~ 5.0	0	-	0	-
10	4MP	HD3	10	4MP	HB3	3.8 ~ 5.6	0	-	0	-
4	DTYR	HA	4	DTYR	HB3	2.6 ~ 3.8	66.7	0.015	0	-
15	MXY	H5	5	CYS	HA	2.8 ~ 4.2	0	-	0	-
11	GLY	HA2	6	THR	HG2#	3.2 ~ 5.8	0	-	0	-
12	TRP	HB#	6	THR	HG2#	3.4 ~ 6.2	0	-	0	-
12	TRP	HE3	3	TRP	HA	2.6 ~ 4.0	0	-	0	-
15	MXY	H3	15	MXY	H8	3.4 ~ 5.2	0	-	0	-
12	TRP	HE3	1	LYS	HB3	3.0 ~ 4.4	8.3	-	33.3	-
3	TRP	HZ2	10	4MP	HB3	2.4 ~ 3.6	8.3	-	0	-
15	MXY	H1	10	4MP	HB3	3.4 ~ 5.2	0	-	0	-
12	TRP	HA	13	THR	HA	3.0 ~ 4.6	0	-	0	-
12	TRP	HB#	13	THR	HA	3.0 ~ 4.6	0	-	16.7	-

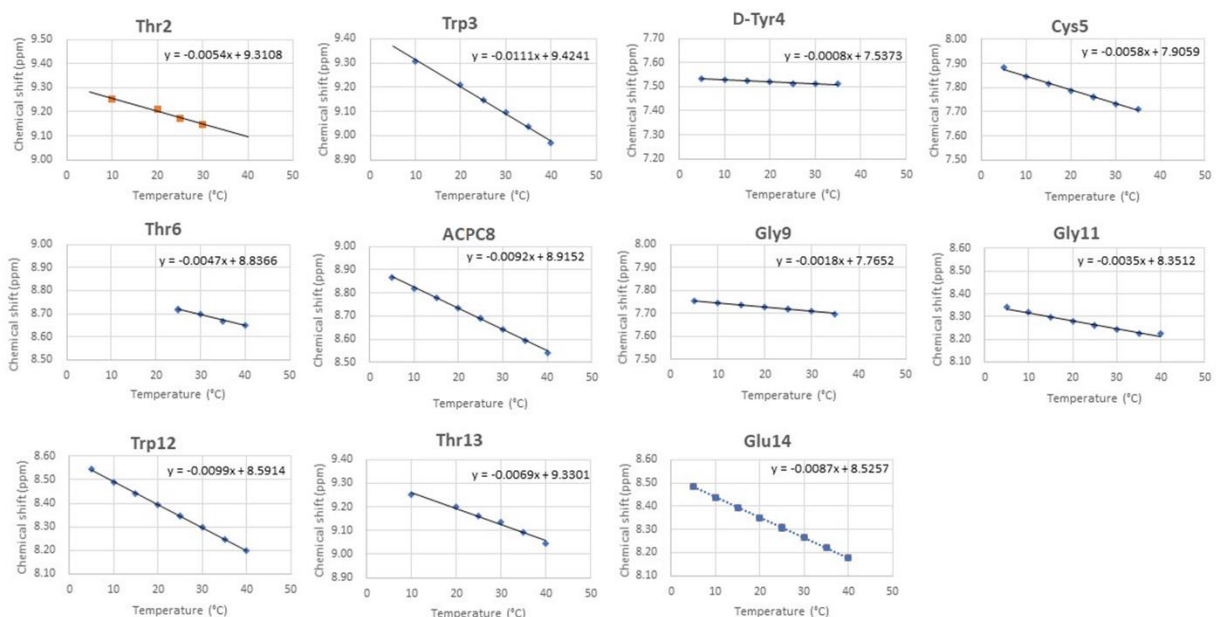


Figure S16. Variable temperature chemical shift data for 4MP-m. Chemical shifts for each amide proton were obtained for temperatures between 5 and 40 degrees Celsius. Linear fits showing slope and intercept are shown.

Table S6. Variable temperature coefficients for amide protons of 4MP-m.

Residue	Amide chemical shift change (ppb/°C)
Lys1	n/a
Thr2	-5.4
Trp3	-11.1
D-Tyr4	-0.8
Cys5	-5.8
Thr6	-4.7
D-Pro7	n/a
ACPC8	-9.2
Gly9	-1.8
4MP10	n/a
Gly11	-3.5
Trp12	-9.9
Thr13	-6.9
Glu14	-8.7

Results from Simulated Annealing

Of the 100 structures produced by simulated annealing, 35 had *cis* peptide bonds and were removed. The remaining 65 structures comprised two well-defined clusters (Figure S17). Cluster 1 (12 structures, Figure S17) largely satisfied the NMR constraints, while Cluster 2 did not, and represents a local minimum accessed repeatedly during the simulated annealing process. Cluster 1 had very few NOE violations (see Table S5 above) and those violations that were observed were all below 0.6 Å. The hydrogen-bonding pattern observed in Cluster 1 is also entirely consistent with the variable temperature NMR data (Table S6 above).

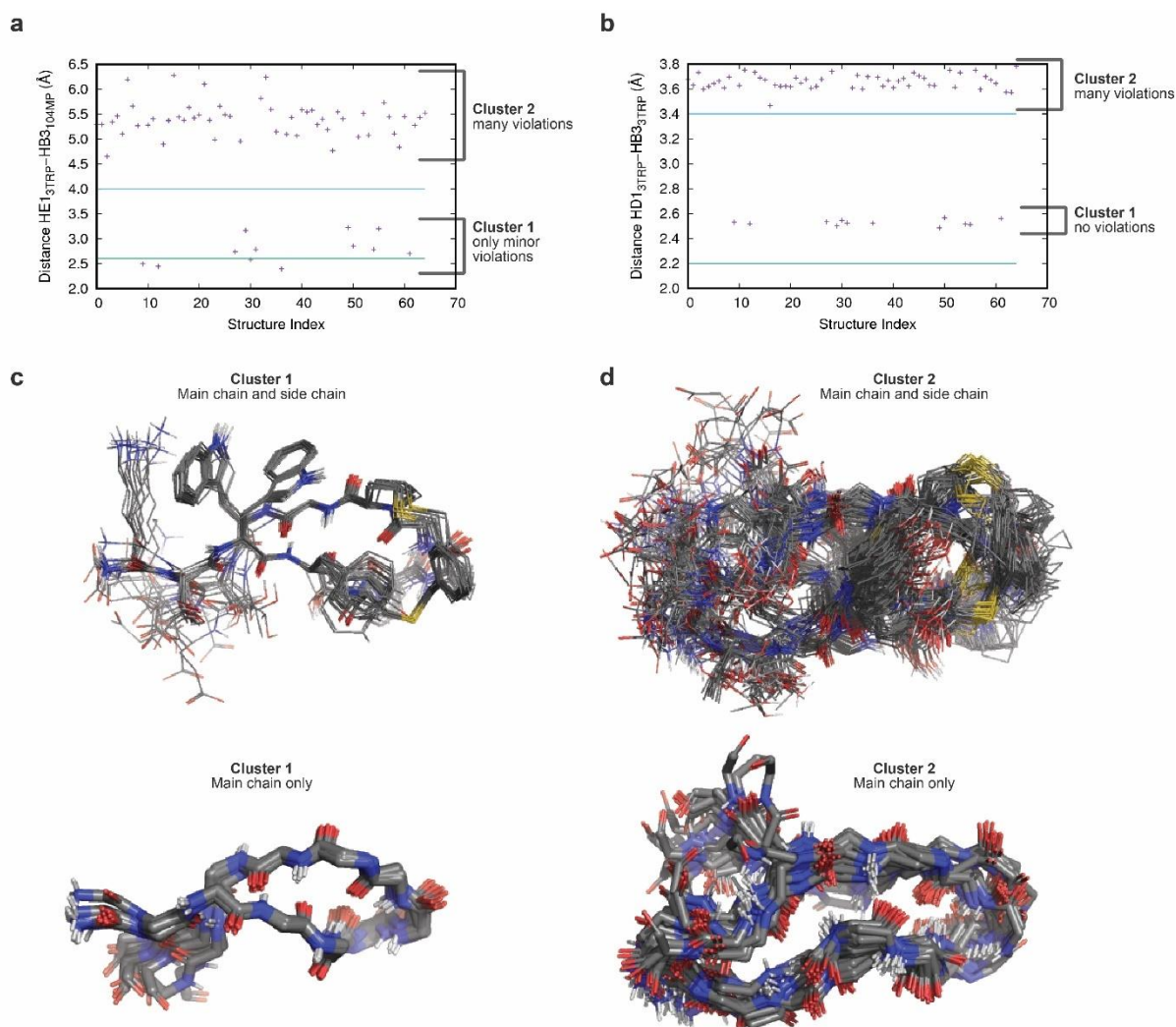


Figure S17. Simulated annealing using NMR constraints produced two distinct clusters.

(a) Proton-proton distances between protons 3HE1 and 10HB3 for the 65 all-*trans* structures that resulted from simulated annealing. (b) Proton-proton distances between protons 3HD1 and 3HB3 for the 65 all-*trans* structures that resulted from simulated annealing. For (a) and (b), the green line and blue line show the lower bound and upper bound, respectively, of the NOE-derived distance restraints. Cluster 1 shows either no violations or only minor violations, while Cluster 2 shows many violations larger than the distances predicted by NOE data. (c) Backbone-overlaid images of the 12 structures in Cluster 1. (d) Backbone-overlaid images of the 53 structures in Cluster 2.

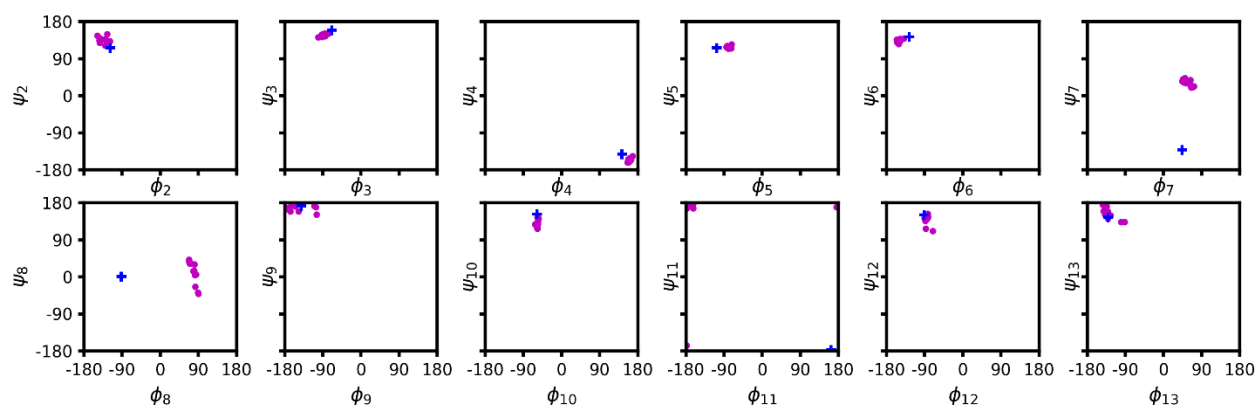


Figure S18. Ramachandran plots for residues 2-13 for the twelve structures in Cluster 1. Blue crosses represent the dihedral angles of the predicted structure, and magenta circles represent dihedral angles observed in Cluster 1. The deviations from the predicted structure for residues 7 and 8 represent the presence of a type I' β -turn instead of the type II' β -turn that was predicted.

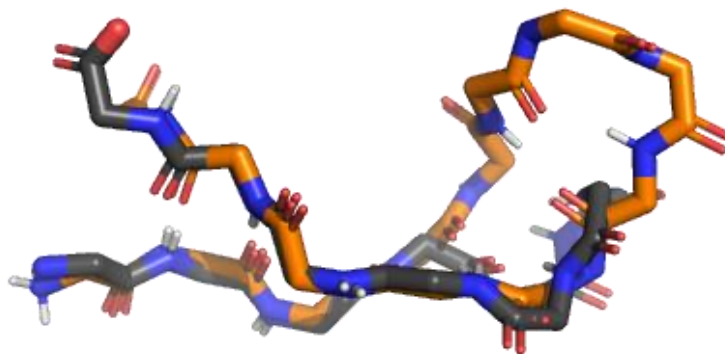


Figure S19. Backbone overlay of 4MP-m with HP7. The designed, stapled hairpin **4MP-m** (orange) overlays well with the model β -hairpin **HP7** (gray) near the termini, but they differ in the regions corresponding to the staple and β -turn.

Alignment analysis comparing 4MP-m and the Protein Data Bank

The potential for the kinked, stapled β -hairpins to mimic natural hairpin structures was assessed by scanning the Protein Data Bank for structurally similar peptide fragments. An input set of protein crystal structures was curated to include high-resolution ($\leq 1.6\text{\AA}$), non-redundant ($\leq 40\%$ sequence identity) structures that contain at least 40 residues. The input set was obtained from the Pisces server (downloaded on 12/02/2020) and it contained a total of 6693 protein chains.¹⁹ For rapid assessment of structural matches, we used a 12-residue fragment of **4MP-m** corresponding to the entire sequence without the N- and C-terminal residues, *TWYCTPXG4GWT*. The backbone coordinates for these 12 residues were aligned with the backbone coordinates of all possible 12-mer fragments within each of the crystal structures in the input set. One set of alignments was performed by aligning first residue of **4MP-m** to the first residue of each 12-mer register, and then calculating the backbone RMSD ("RMSD terminal"). For completeness, a second set of alignments was performed by aligning sixth residue of **4MP-m** to the sixth residue of each 12-mer register, and then calculating the backbone RMSD ("RMSD turn"). PDB manipulation and calculations were done using the AMPAL Python package.²⁰ All 187 alignments with backbone RMSD values below 2.0\AA are listed in Table S7, and selected examples are shown in Figure S20.

Additionally, we sought to estimate the potential for 4MP-m and related hairpins to serve as scaffolds for inhibitors of protein-protein interactions. As an initial estimate, we analyzed each 12-residue fragment in Table S7 for their proximity to a protein-protein interface. Residues within each sequence that reside within 4\AA of another chain in the complex are noted in Table S7, and selected examples are shown in Figure S21.

Table S7. Alignments with calculated RMSD values below 2.0\AA for **4MP-m** and peptide fragments identified in the Protein Data Bank.

PDB_ID	Chain	Start	Finish	Sequence	PPI Sequence*	RMSD terminal (\AA)	RMSD turn (\AA)
1DCS	A	204	215	LQAEVGGAFSDL			1.907
1E9G	A	58	69	EITKEETLNPII	-----	1.962	
1EU1	A	8	19	VMSGCHWGVFKA		1.816	
1EW4	A	70	81	HFDLKGDEWICD			1.694
1GQI	A	104	115	EQTRINKRHVVI	-----	1.503	
1K3X	A	245	256	EKTTLSRRPFYW	-----		1.908
1KB0	A	318	329	ADIKIAGKPRKV		1.831	
1L6R	A	134	145	VIFYSGYSWHLM	V-----	1.885	
1MXR	A	173	184	GHTVNGKTVTV	--HTVNG----	1.876	
1N7O	A	394	405	GSYIDHTNVAYT			1.996
1OH4	A	38	49	EWNGEVNGALQ	-----	1.809	
1OLR	A	139	150	SQVNLARGTWDL		1.859	
1PMH	X	128	139	KKVKINGKDYTV	-----	1.685	
1QS1	A	222	233	GVILNNSEYKML	-----		1.676
1QS1	A	246	257	SKVVKKGVECLQ	-----	1.967	
1T1G	A	263	274	YEVVIDGETTVI		1.421	
1T9H	A	210	221	ELIHTSGGLVAD			1.964

1UK8	A	8	19	KSILAGVLTNY		1.811	
1UOY	A	35	46	VVECKGGKWTEV			1.657
1UTI	A	37	48	WTGRLHNKLGFL	-----	1.635	
1V30	A	84	95	VEVSTKFGKAFL		1.961	
1V5V	A	20	31	KIEEFAGWEMPI	-----AG-----		1.821
1V5V	A	182	193	RWVELDGIKMLL	-----	1.972	
1V5V	A	194	205	SRSGYTGENGFE	-----	1.632	
1W0P	A	56	67	VLTNADGMPAWL		1.993	
1W70	A	208	219	LEGTVRGATGIF	-----	1.514	
1WCU	A	28	39	KMSFKDNSLVLT		1.925	
1X6O	A	32	43	GYVCINGRPCKV		1.903	
1Y2M	A	233	244	VHVHVEGKEKIL	-----	1.435	1.756
2BMO	A	53	64	VKAKMGVDEVIV	-----	1.994	
2BW8	A	143	154	ATVELAGATWEV	-----		1.907
2DPL	A	239	250	TVGVQGDIRAYK	TV-V-----Y-	1.933	
2DVM	A	217	228	VVELVNGKPRIL	-----		1.398
2EBB	A	19	30	GWKLADERWIVK			1.564
2G6F	X	44	55	WEGTHNGRTGWF		1.185	
2H5C	A	45	53	FSVTRGATKGFV		1.752	
2ICI	A	40	51	KNIPYGNSSIEL			2.000
2IWR	A	108	119	KEMLVDGQTHLV		1.642	
2JEN	A	173	184	ETVSIGGHSWKV	-----	1.837	1.848
2PQC	A	292	303	NPRLAGGEDVAD			1.615
2QIK	A	84	95	VFVETDVGIIA		1.681	
2R9F	A	151	162	FQLWQFGEWVDV		1.524	1.499
2VXT	I	162	173	AAEKERDLFKLI	-----	1.989	
2W1V	A	123	134	IPEEDAGKLYNT	-----	1.656	
2WFW	A	95	106	VDVFTSGRKML	-----	1.401	1.682
2WRY	A	79	90	SCVMSGTEPTLQ		1.592	
2XGU	A	1	12	PIMLRGGRQEYE	-----		1.876
3ACH	A	53	64	TIKDANESKAIS	-----	1.345	1.961
3AKS	A	6	17	GTGYNNGYFYSY		1.673	
3AMN	B	10	21	SDFVWNGIPLSM	-----	1.984	
3AMR	A	91	102	ASNRSEGKNTIE		1.793	
3AMR	A	309	320	GENIDHGQKANQ			1.937
3BMZ	A	124	135	GRRVVLGREADG	--RVVLG-----		1.974
3C8W	C	91	102	VPVRYKGEEGGF	-----	1.461	
3CB0	A	160	171	ALIYLNRRYHKL	-----	1.775	
3DUW	A	205	216	LQTVGSKGYDGF	LQTVG---Y--F	1.803	
3FSS	A	222	233	LQCHRGTKEGTL		1.649	
3G48	A	21	32	EEFKEARVPAIR	E-F-----R	1.299	
3GNE	A	30	41	AVTTFDGKRUVK	-----	0.788	1.348
3GZX	A	74	85	LTTYMGEDPVIM	-----	1.917	

3HUH	A	48	59	SAVTFKQNRKAL	-----		1.804
3I45	A	344	355	RTALRDGKGMV		1.863	
3IRP	X	780	791	DVVFENGRIYIAH			1.826
3JSY	A	150	161	PAAIEKGKIAIK	-----		1.302
3JU4	A	803	814	IRASTSSNIRSE			1.907
3MDM	A	75	86	VRVNVFHKTSVI		1.802	1.835
3MWX	A	6	17	EKITYLGTPAIK	EK-----	1.665	
3NGP	A	42	53	WKIEVNGRQGFV		1.880	
3O12	A	94	105	GIEISDGHAXLS			1.889
3PB6	X	137	148	FTASTPLGPVDF		1.863	
3PES	A	5	16	FEDRVAGIPCLI	F-----	1.689	
3PME	A	875	886	SLQNKKNALVDT			1.837
3PME	A	1114	1125	YIAPKNNILVLV		1.982	
3QZR	A	16	27	RQVQTDQGHFTM	-----	1.739	
3R4Z	A	209	220	CLMFFNNRFYLY	-----		1.663
3RR6	A	4	15	GRIASPDGVAFV		1.768	
3SC7	X	342	353	SLKKVGTQQHFV	-----	1.923	
3SLZ	A	69	80	RKVHLATGKVTH	-----	1.753	
3VGI	A	219	230	VPIIVNGTPVNA		1.324	
3WEO	A	492	503	YKINNSGGRVPI	-----		1.811
3WP4	A	132	143	GSFTIDGAQYTV			1.600
3ZTV	A	54	65	TRINLNGQQTKV		1.705	
3ZYP	A	100	111	RIGGQSQVLDYN			1.558
4BPS	A	50	61	DVSLVDGAPRTA		1.785	
4CC2	A	1555	1566	WLAEVNGKKGYV	-----	1.619	
4DWR	A	335	346	EEHEVDGKRKV	-----	1.667	
4E2U	A	33	44	GELPFDNGYAVP			1.955
4EQP	A	23	34	VKLMYKGQPMTF		1.466	
4F06	A	364	375	EVEKVDGKLINR		1.448	
4FR9	A	63	74	ADCQADGREXEV			1.668
4GVQ	A	66	77	VVDTINDVPFAF	-----	1.600	
4JG2	A	136	147	YAFNSNGNKGVA		1.540	
4JHT	A	68	79	GWTTTHRQGYLYS		1.133	1.362
4LGY	A	394	405	EKVNSHNGEELR		1.383	
4LUK	A	171	182	IVIEENGVEKVV		1.626	
4PH8	A	134	145	VDFDNKQGGASQ		1.986	
4PI8	A	55	66	QTKEEDGKFVEA	-----		1.764
4PIT	D	79	90	EVANYTGAVVLG	-----		1.436
4QLP	A	44	55	FIDRLAGWYVIT	F-----		1.526
4QLP	A	112	123	GTMTFAGRQRDT	-----RQRD-	1.576	1.829
4R52	A	68	79	LNLWVDGRRERA			1.768
4RD4	A	259	270	LRVEKQGKVSYE		1.252	
4RD7	A	10	21	NLRLDNNLRAQR			1.856

4W6Y	A	68	79	ILVWKNRETQY	-----	1.803	
4WCK	A	348	359	VKMQIDNKDQMV		1.491	
4WHS	C	173	184	KRCEVDGKTAYR	-----	1.777	
4WY9	A	184	195	IKMNLEGQDFDA		1.687	
4XHY	A	165	176	PLVFAAGRFGQF			1.877
4XJW	A	423	434	SVDFDSGSLRER		1.830	
4YG0	A	117	128	VTNVNMNETVNI	-----	1.905	
4YTB	A	134	145	WFAMYDTNKVGL			1.686
4Z4D	A	205	216	SVRPSLWKMLLN	-----	1.578	
4ZUR	B	15	26	KTELYGGELVPP	-T-LYGGEL---		1.670
5A10	A	313	324	TTTTINGKKGLL		1.194	
5A57	A	904	915	VTMTDNGSTYKW		1.595	
5BOW	A	19	30	ALYTRDQQLLVG		1.870	
5C17	A	89	100	NQIHLGGRTLFA			1.762
5D7W	A	309	320	SFSDVGGLKGNV			1.757
5DGJ	A	8	19	RVTKFGSGWGF			1.941
5DGJ	A	105	116	ASMRIQGRLVHG		1.451	
5EX2	A	118	129	YTGfYNGFPiET	-----	1.948	
5G28	A	75	86	AYAYVDGSYQLQ			1.838
5GTQ	A	71	82	FVVSLEIEAIL		1.675	
5HT2	A	221	232	VNVSLGGNEFCL	-----	1.984	
5I0Y	A	88	99	MPMVASDGPHYG	MPMVASDGPHY-	1.726	
5K26	A	84	95	WAGQVGGQVGIF	W-----	1.317	
5K7A	A	49	60	TPLAIAGQRATL		1.330	1.489
5L20	A	91	102	ELAYENGKSVHK	-----		1.869
5MBX	A	47	58	RSERCFGVVEL			1.745
5MC7	A	58	69	EIALLEGLTVVY	-----		1.702
5MK9	A	253	264	PTIKLDGKDVQM	-----		1.864
5MUA	B	116	133	FVTLLNGTVVGW	-----	1.303	
5N4B	A	363	374	QVNCANEEYFVA	-----		1.999
5NVJ	A	41	52	WRGVCKGRYGLF	---V-KGRY---	1.207	
5O99	B	508	519	WEGTVKGRWGWF	-----K-R----	1.426	
5OAZ	A	100	111	CEAQTKNGQGWV	-E-QTK-GQ---	1.917	
5OXZ	A	7	18	IEVIENGIKKKE	IE-----K-	1.275	
5R8Q	A	70	81	SCVLKDDKPTLQ		2.000	
5T5L	A	21	32	GASPRNETLQLT	-----		1.859
5TNW	B	704	715	ISFRAEGKIKHC	-----KIKH-		1.765
5UMS	A	341	352	ITCSYKASSGLL		1.442	
5VFB	A	192	203	SYSVKNGALVVA	-----		1.993
5VOG	A	63	74	YDSDNEGQVTEE		1.741	
5X4B	A	44	55	SSAEWLNYDFNL	----WL-----	1.918	
5XZ7	A	285	296	GVGIKNNKIVAT		1.764	
5YKJ	A	58	69	FDADTTVGKINF		1.883	

5YQJ	A	822	833	KTPGAIGPGKT	-----	1.569	
5YZP	A	392	403	HLKTIDRQPKLV		1.888	
6B26	A	330	341	WKGKIGDRVGGF		1.815	
6B26	A	392	403	IRVSSGKKRGLV		1.799	
6BCD	A	43	54	QARKKYNVPVQM	-----		1.880
6DGA	A	66	77	LSLSLFGELVPV		1.930	
6DGG	A	187	198	RWIKTRKGQRLF		1.907	
6EWM	A	163	174	EFSHGPAGPTYK	EFSHGP-GP---	1.366	
6FBQ	A	142	153	SSGKHVGVYSCE	-----		1.666
6FU9	B	76	87	MDMKVGNVWHI	-----	1.819	
6FYJ	A	39	50	FETRLLGKKAIC		1.523	1.629
6G00	A	175	186	ITGPTNRGVMTA		1.896	
6GDY	B	49	60	SCYRWQGAIARE	-----		1.907
6I05	A	298	309	SSVVRNQILHR			1.822
6JVV	A	2	13	RLARFDGGRGLV	-----		1.927
6JYZ	A	36	47	RLTVEDGAIKDV			1.975
6KIA	B	244	255	TEILIDDKYQWQ	-----		1.927
6LF2	B	61	72	FLQYNGEQVIMS	-----	1.702	
6LF2	B	103	114	YLDYNGGDLVAN	-----	1.985	
6NP3	A	207	218	MPLLREGKRVWV		1.934	
6PNV	A	305	316	FTSDQAGRPQVY		1.504	
6PNV	A	349	360	MVSSNNGQQHIA		1.691	
6QLA	B	74	85	RHETLNAVHVQV	-----	1.647	
6R1G	B	112	123	APISISGKEAFI	-----	1.639	
6RK0	A	45	56	VGCMNGVPFVVT	VGCM-NGVPFVVT	1.974	
6RPP	A	96	107	FFVLEEGKVAMR		1.618	
6SQX	B	199	210	TLIKGQGTGLGW	-----	1.386	
6SQX	B	401	412	GTTEYNHNKVAI	----YN-----		1.927
6ST4	A	44	55	VLCNSTTTFNE		1.939	
6SXT	A	363	374	YIAHTDTTVNTQ	-----	1.859	
6SXT	A	413	424	YIRHYNFELLN	-----	1.693	
6SXT	A	460	471	YFRHYENVLYAA	-----	1.883	
6SYI	A	548	559	MLLRTAIGQVSR	-----	1.755	
6UT9	A	54	65	RQYVLFGENKQF		1.924	
6V42	B	366	377	EFVRFDDGDI	---RFDGDI---	1.573	1.871
6VHU	A	372	383	ITIPYQGTMLF	-----	1.820	
6VTB	A	69	80	QVIDYEGQRGTR			1.778
6WFN	A	62	73	RVDHSQNQKRLY		1.327	
6Y43	A	274	285	YELRVGRHVSV		1.995	
6YP6	A	540	551	YIQTDAKDLNVM		1.939	
7KPO	A	1063	1074	RVYLDRLTLQTR			1.369

*One-letter amino acid codes are shown for residues within each sequence that reside within 4 Å of another chain in the complex. All dashes indicates that no residues reside within 4 Å of another chain, and no dashes indicate a single-chain complex.

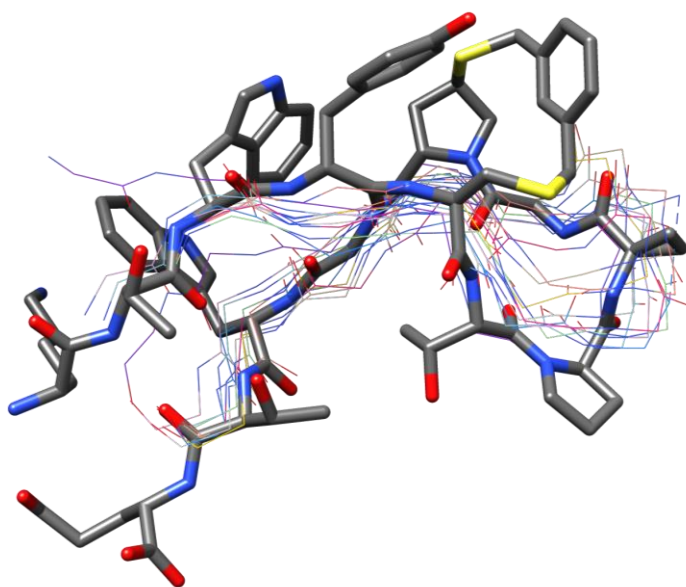


Figure S20. 4MP-m aligns with β -hairpin structures in the Protein Data Bank. Solution structure of **4MP-m** overlaid with the 12-residue protein fragments with the lowest backbone RMSD values (Table S7). Overlaid structures include 3GNE, 4JHT, 2G6F, 5A10, 5NVJ, 4RP4, 5OXZ, 3G48, 3JSY, and 5MUA.

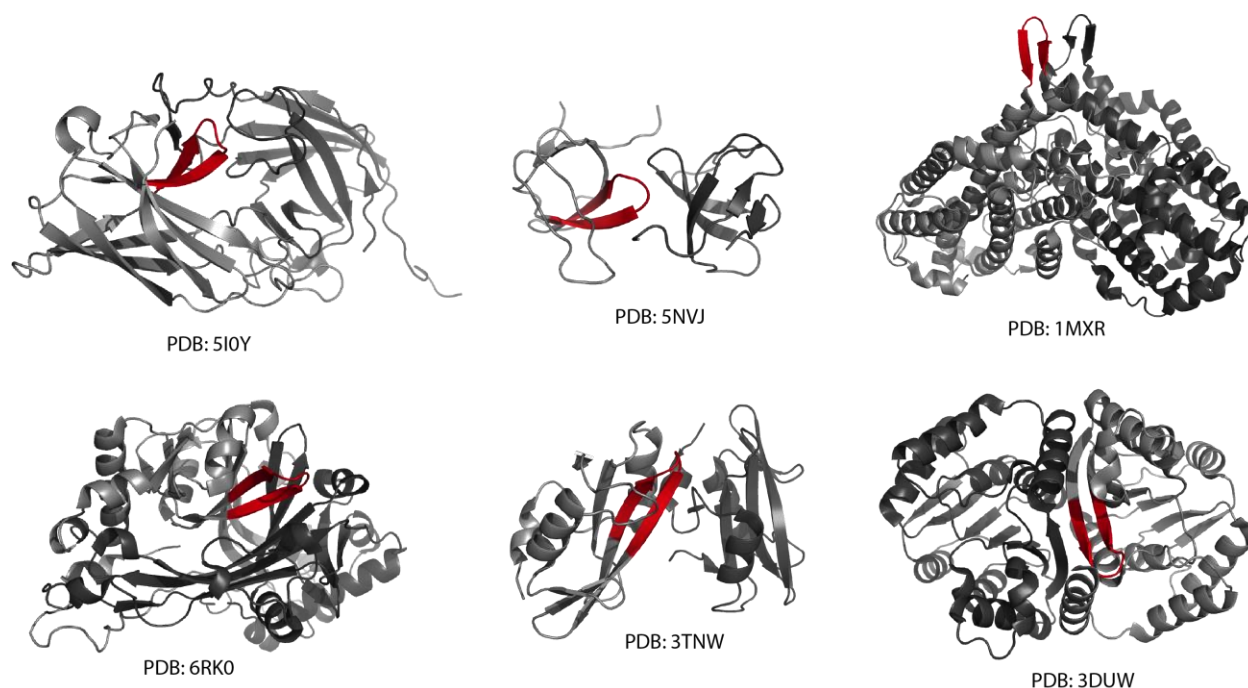


Figure S21. 4MP-m aligns with β -hairpin structures at protein-protein interaction interfaces. Representative examples of β -hairpin structures in the PDB that align well with **4MP-m** (backbone RMSD under 2.0 Å) and that reside at protein-protein interactions. 12-residue fragments that align with **4MP-m** are shown in red.

References

- (1) Peraro, L.; Deprey, K. L.; Moser, M. K.; Zou, Z.; Ball, H. L.; Levine, B.; Kritzer, J. A. Cell Penetration Profiling Using the Chloroalkane Penetration Assay. *J. Am. Chem. Soc.* **2018**, *140* (36), 11360–11369.
- (2) Deprey, K.; Kritzer, J. A. Quantitative Measurement of Cytosolic Penetration Using the Chloroalkane Penetration Assay. *Meth. Enzymol.* **2020**, *641*, 277–309.
- (3) Timmerman, P.; Beld, J.; Puijk, W. C.; Meloen, R. H. Rapid and Quantitative Cyclization of Multiple Peptide Loops onto Synthetic Scaffolds for Structural Mimicry of Protein Surfaces. *ChemBioChem* **2005**, *6* (5), 821–824.
- (4) Peraro, L.; Siegert, T. R.; Kritzer, J. A. Conformational Restriction of Peptides Using Dithiol Bis-Alkylation. *Meth. Enzymol.* **2016**, *580*, 303–332.
- (5) Gomis-Rüth, F. X.; Dessen, A.; Timmins, J.; Bracher, A.; Kolesnikowa, L.; Becker, S.; Klenk, H.-D.; Weissenhorn, W. The Matrix Protein VP40 from Ebola Virus Octamerizes into Pore-like Structures with Specific RNA Binding Properties. *Structure* **2003**, *11* (4), 423–433.
- (6) Hosseinzadeh, P.; Bhardwaj, G.; Mulligan, V. K.; Shortridge, M. D.; Craven, T. W.; Pardo-Avila, F.; Rettie, S. A.; Kim, D. E.; Silva, D.-A.; Ibrahim, Y. M.; Webb, I. K.; Cort, J. R.; Adkins, J. N.; Varani, G.; Baker, D. Comprehensive Computational Design of Ordered Peptide Macrocycles. *Science* **2017**, *358* (6369), 1461–1466.
- (7) Diener, M. E.; Metrano, A. J.; Kusano, S.; Miller, S. J. Enantioselective Synthesis of 3-Arylquinazolin-4(3H)-Ones via Peptide-Catalyzed Atroposelective Bromination. *J. Am. Chem. Soc.* **2015**, *137* (38), 12369–12377.
- (8) Hurtley, A. E.; Stone, E. A.; Metrano, A. J.; Miller, S. J. Desymmetrization of Diarylmethylamido Bis(Phenols) through Peptide-Catalyzed Bromination: Enantiodivergence as a Consequence of a 2 Amu Alteration at an Achiral Residue within the Catalyst. *J. Org. Chem.* **2017**, *82* (21), 11326–11336.
- (9) Sawyer, N.; Arora, P. S. Hydrogen Bond Surrogate Stabilization of β -Hairpins. *ACS Chem. Biol.* **2018**, *13* (8), 2027–2032.
- (10) Kaminski, G. A.; Friesner, R. A.; Tirado-Rives, J.; Jorgensen, W. L. Evaluation and Reparametrization of the OPLS-AA Force Field for Proteins via Comparison with Accurate Quantum Chemical Calculations on Peptides. *J. Phys. Chem. B* **2001**, *105* (28), 6474–6487.
- (11) Jorgensen, W.; Chandrasekhar, J.; Madura, J.; Impey, R.; Klein, M. Comparison of Simple Potential Functions for Simulating Liquid Water. *J. Chem. Phys.* **1983**, *79* (2), 926–935.
- (12) Bussi, G.; Donadio, D.; Parrinello, M. Canonical Sampling through Velocity Rescaling. *J. Chem. Phys.* **2007**, *126* (1), 014101.
- (13) Berendsen, H. J. C.; Postma, J. P. M.; van Gunsteren, W. F.; DiNola, A.; Haak, J. R. Molecular Dynamics with Coupling to an External Bath. *J. Chem. Phys.* **1984**, *81* (8), 3684–3690.
- (14) Hockney, R. W.; Goel, S. P.; Eastwood, J. W. Quiet High-Resolution Computer Models of a Plasma. *Journal of Computational Physics* **1974**, *14* (2), 148–158.
- (15) Hess, B.; Bekker, H.; Berendsen, H. J. C.; Fraaije, J. G. E. M. LINCS: A Linear Constraint Solver for Molecular Simulations. *Journal of Computational Chemistry* **1997**, *18* (12), 1463–1472.
- (16) Darden, T.; York, D.; Pedersen, L. Particle Mesh Ewald: An $N \cdot \log(N)$ Method for Ewald Sums in Large Systems. *J. Chem. Phys.* **1993**, *98* (12), 10089–10092.
- (17) Essmann, U.; Perera, L.; Berkowitz, M. L.; Darden, T.; Lee, H.; Pedersen, L. G. A Smooth Particle Mesh Ewald Method. *J. Chem. Phys.* **1995**, *103* (19), 8577–8593.
- (18) Ballister, E. R.; Aonbangkhen, C.; Mayo, A. M.; Lampson, M. A.; Chenoweth, D. M. Localized Light-Induced Protein Dimerization in Living Cells Using a Photocaged Dimerizer. *Nat Commun* **2014**, *5* (1), 1–9.

- (19) Wang, G.; Dunbrack, R. L. PISCES: A Protein Sequence Culling Server. *Bioinformatics* **2003**, *19* (12), 1589–1591.
- (20) Wood, C. W.; Heal, J. W.; Thomson, A. R.; Bartlett, G. J.; Ibarra, A. Á.; Brady, R. L.; Sessions, R. B.; Woolfson, D. N. ISAMBARD: An Open-Source Computational Environment for Biomolecular Analysis, Modelling and Design. *Bioinformatics* **2017**, *33* (19), 3043–3050.